Bioorganic Chemistry 150 (2024) 107588

Contents lists available at ScienceDirect

Bioorganic Chemistry

journal homepage: www.elsevier.com/locate/bioorg

Synthesis and anti-proliferative effect of novel 4-Aryl-1, 3-Thiazole-TPP conjugates via mitochondrial uncoupling process

Yixin Hu [a], Yang Zhang [a], Jie Guo [b], Shihao Chen [b], Jie Jin [b], Pengyu Li [b], Yuchen Pan [b], Shuwen Lei [a], Jiaqi Li [b], Suheng Wu [b], Buzhou Bu [b], Lei Fu [a,b,*]

[a] Shanghai Key Laboratory for Molecular Engineering of Chiral Drugs, School of Pharmacy, Shanghai Jiao Tong University, Shanghai, China
[b] Academy of Pharmacy, Xi'an Jiaotong-Liverpool University, Suzhou, China

ARTICLE INFO

Keywords:
Anticancer
Mitochondrial targeting
Oxidative phosphorylation
Mitochondrial bioenergetics
Mitochondrial uncoupler

ABSTRACT

With the advent of mitochondrial targeting moiety such as triphenlyphosphonium cation (TPP^+), targeting mitochondria in cancer cells has become a promising strategy for combating tumors. Herein, a series of novel 4-aryl-1,3-thiazole derivatives linked to TPP^+ moiety were designed and synthesized. The cytotoxicity against a panel of four cancer cell lines was evaluated by CCK-8 assay. Most of these compounds exhibited moderate to good inhibitory activity over HeLa, PC-3 and HCT-15 cells while MCF-7 cells were less sensitive to most compounds. Among them, compound **12a** exhibited a significant anti-proliferative activity against HeLa cells, and prompted for further investigation. Specifically, **12a** decreased mitochondrial membrane potential and enhanced levels of reactive oxygen species (ROS). The flow cytometry analysis revealed that compound **12a** could induce apoptosis and cell cycle arrest at G0/G1 phase in HeLa cells. In addition, mitochondrial bioenergetics assay revealed that **12a** displayed mild mitochondrial uncoupling effect. Taken together, these findings suggest the therapeutic potential of compound **12a** as an antitumor agent targeting mitochondria.

1. Introduction

Mitochondria are essential organelles in eukaryotic cells. Their most critical role is to produce the energy-rich molecule adenosine triphosphate (ATP) via oxidative phosphorylation (OXPHOS) and tricarboxylic acid (TCA) cycle. Mitochondria are therefore considered as "power house" of cells [1]. Mitochondria also play critical role in generation of reactive oxygen species (ROS), and regulation of cell signaling and death [2]. Recent findings showed that mitochondrial TCA cycle metabolites control both physiology and disease [3]. Given the important role of mitochondria, it is expected that the dysfunction and disorder of mitochondria is associated with various diseases, including cardiovascular disease [4], neurodegenerative disease [5,6], metabolic diseases [7–9] and cancers [10–12].

For a long time, mitochondrial metabolism has been viewed as inconsequential to the proliferation of cancer cells. Warburg stated that cancer cells undergo aerobic glycolysis in the presence of ample oxygen which is referred to the Warburg effect [13]. As a result, mitochondrial dysfunction and aerobic glycolysis have been widely recognized as hallmarks of cancer [14]. However, the belief that mitochondrial metabolism was dispensable for tumor proliferation was challenged recently. A number of notable differences in the structure and function of mitochondria between cancer and normal cells have been reported [15]. In addition, accumulating evidence revealed that mitochondrial bioenergetics, biosynthesis and signaling are involved for tumorigenesis [16].

Delocalized lipophilic cations tend to accumulate inside mitochondria against concentration gradient because of the negative mitochondrial inner membrane potential (−180 mV)] [17]. The triphenylphosphonium cation (TPP^+) is the most widely used delocalized lipophilic cation as mitochondrial targeting moiety due to its high lipophilicity and bio-inertness [18]. In addition, the mitochondrial membrane potential (MMP) of cancer cells is more negative (about −220 mV) than that of normal cells [19,20], which allows molecules containing TPP^+ to target tumor mitochondria selectively. As reported, some natural products including artemisinin, curcumin, botulin and camptothecin [21–24] as well as approved drugs, such as chlorambucil, phenylbutyric acid and ciprofloxacin (CFX) [25–27] were coupled with TPP^+ to improve their anticancer selectivity and activity. Representative examples are illustrated in Fig. 1A. Besides, a small library of 2-arly-1,3-

* Corresponding author at: Academy of Pharmacy, Xi'an Jiaotong-Liverpool University, Suzhou, China.
E-mail address: lei.fu@xjtlu.edu.cn (L. Fu).

https://doi.org/10.1016/j.bioorg.2024.107588
Received 11 May 2024; Received in revised form 18 June 2024; Accepted 22 June 2024
Available online 23 June 2024

thiazole-TPP conjugates exhibiting anticancer activity *in vitro* and *in vivo* was prepared in our previous research (e.g. Fig. 1B) [28,29].

A few researches revealed that different length of linkers had impact on the activities of TPP^+ conjugates by modulating lipophilicity and the cell region to be accumulated [30–32]. Base on the above findings, a novel series of 4-aryl-1,3-thiazole derivatives bearing longer linkers were designed and synthesized (Fig. 2). Among the new family of compounds, **12a** exhibited most potent anti-proliferative activity, decreased mitochondrial membrane potential and increased reactive oxygen species (ROS) production. Moreover, compound **12a** induced apoptosis and displayed mitochondrial uncoupling effect.

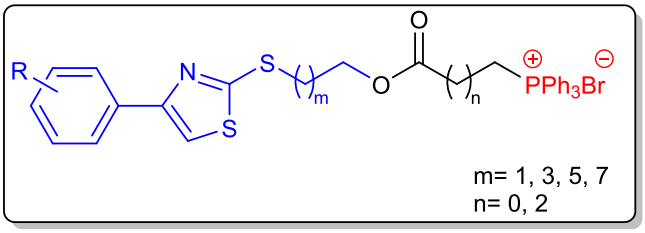

Fig. 2. Design of Novel Mitochondrial Targeting 4-Aryl-1,3-Thiazole-TPP Conjugates.

2. Results and discussion

2.1. Chemistry

According to the Hantzsch thiazole synthesis, a set of thiazole-2-thiols (**2a-2k**) with substituents on the phenyl ring were prepared by condensing arylbromoketones **1a-1k** and ammonium carbamodithioate under reflux [33]. Then, **2a-2k** reacted with 2-bromoethanol to give the corresponding compounds **3a-3k** under mild basic condition and room temperature. Esters **4a-4k** were obtained by reacting bromoacetyl bromide and compounds **3a-3l** in ice bath. The final triphenylphosphoniums **5a-5k** were prepared through treating esters **4a-4k** with triphenylphosphine under room temperature (Scheme 1). Compounds **8a** and **8b** were synthesized according to synthetic route depicted in Scheme 2. Specifically, 2-bromo-4′-hydroxyacetophenone was reacted with ammonium carbamodithioate under reflux to give thiazole-2-thiol **2l** which underwent a nucleophilic substitution reaction with 2-bromoethanol to yield intermediate **3l**. Benzyl bromide bearing different substituent was reacted with intermediate **3l** giving compounds **6a** and **6b** under room temperature. Compounds **6a** and **6b** were finally converted to compounds **8a** and **8b** through similar reactions referring the preparation of compounds **5a-5k**. In order to investigate how the length of the linker affect the activities, compounds **9a-9f** and **12a-12c** were prepared respectively (Scheme 3 and Scheme 4). In the case of **9a-9f**, distance between ester group and TPP^+ was extended from one carbon to three carbons, comparing to compounds **5a-5k**. The formation of compounds **9a-9f** was achieved by condensation of alcohols **3a-3c**, **3h-3j** and (3-carboxypropyl) triphenylphosphonium bromide in the presence of 1-ethyl-3-(3-dimethylaminopropyl) carbodiimide (EDCI) and DMAP. The linkers of compounds **12a-12c** were extended by prolonging the carbon chain between 1,3-thiazloe ring and ester group. Thiazole-2-thiol **2c** was treated with different bromo-alchol under mild basic condition to give compounds **10a-10c** followed by reacting with bromoacetyl bromide to offer the corresponding esters **11a-11c**. Compounds **12a-12c** were finally obtained by reacting with triphenylphosphine overnight under room temperature.

2.2. In vitro cytotoxic activity (CCK-8 assay)

The newly synthesized 4-aryl-1,3-thiazole-TPP conjugates (**5a-5k, 8a-8b, 9a-9f** and **12a-12c**) were screened for their cytotoxicity against four human cancer cell lines viz. HeLa (cervical cancer), PC-3 (prostate cancer), MCF-7 (breast cancer) and HCT-15 (colon cancer) using CCK-8 assay. **12a-12c** were also tested on a normal cell line BEAS-2A (bronchial epithelial cell). The concentration causing 50 % inhibition of cancer cell growth are expressed as IC_{50} values. Doxorubicin, Dasatinib and CCCP were used as positive controls. The IC_{50} values of tested compounds are listed in Table1. Firstly, different substituents including halogen atoms, electron donating groups (EDG) and electron withdrawing groups (EWG) were introduced on the phenyl ring (**5a-5k, 8a, 8b**). As shown in Table 1, compared to unsubstituted **5a**, compounds bearing chlorine and bromine group at 4- position and 3- position (**5c-5f**) exhibited good inhibitory activity over four tested cancer cell lines. Whereas, *para*-fluorine (**5b**), EDG including *para*-methyl (**5g**), *para*-methoxy (**5f**) groups and EWG including *para*-trifluoromethyl (**5i**), *para*-cynao (**5j**), *para*-nitro (**5k**) groups decreased their inhibitory activity to varying degrees. Analogs containing *para*-benzyloxy and 4-Cl-benzyloxy groups (**8a**, **8b**) exerted moderate to good inhibitory effect against PC-3 and HCT-15 cells while less potency against HeLa and MCF-7 cells showing IC_{50} higher than 50 μM.

Next, we investigated how the linkers between 1,3-thiazole ring and TPP^+ affect the efficacy of our compounds. When the length of carbon chain between TPP^+ and ester group was increased from one carbon atom to three carbon atoms, the anti-proliferative activity of compounds

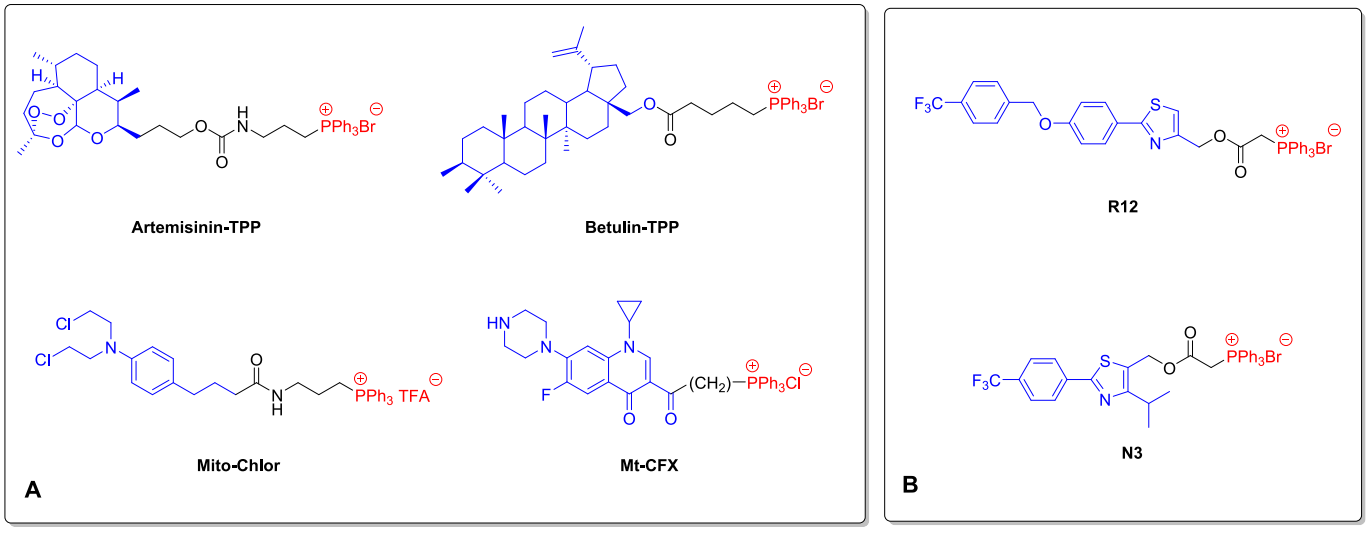

Fig. 1. Chemical structures of reported TPP based anticancer agents.

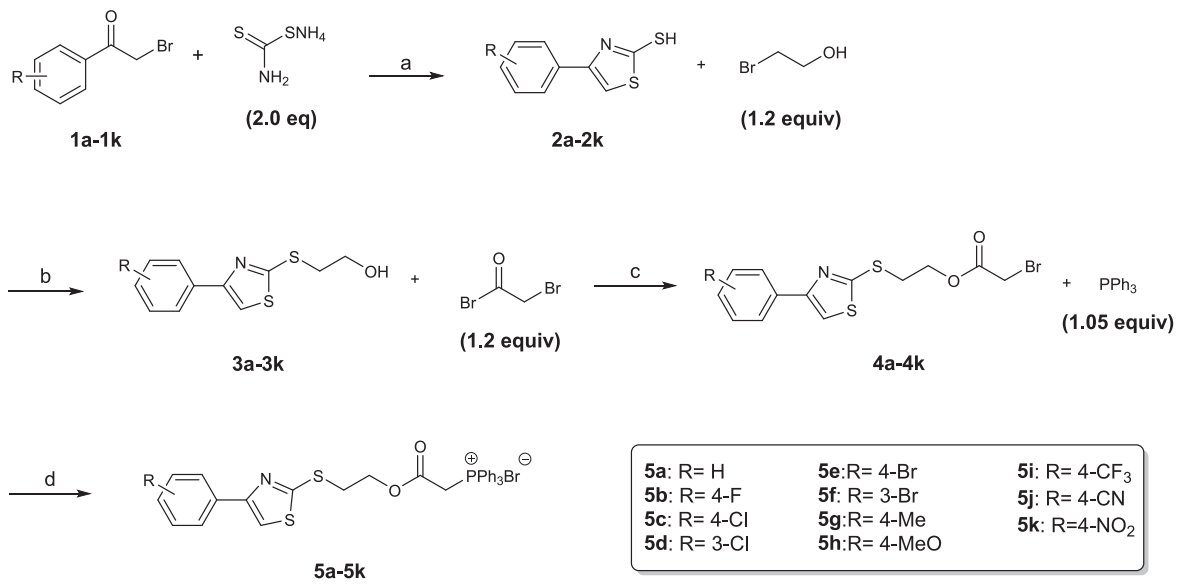

Scheme 1. Synthesis of **5a**-**5 k**. Reaction conditions: a: EtOH, H_2O, 0 °C to 80 °C, 3 h. b: K_2CO_3 (1.2 equiv), acetone, rt, 4 h. c: DCM or THF, 0 °C to rt, 2 h. d: CH_3CN, rt, overnight.

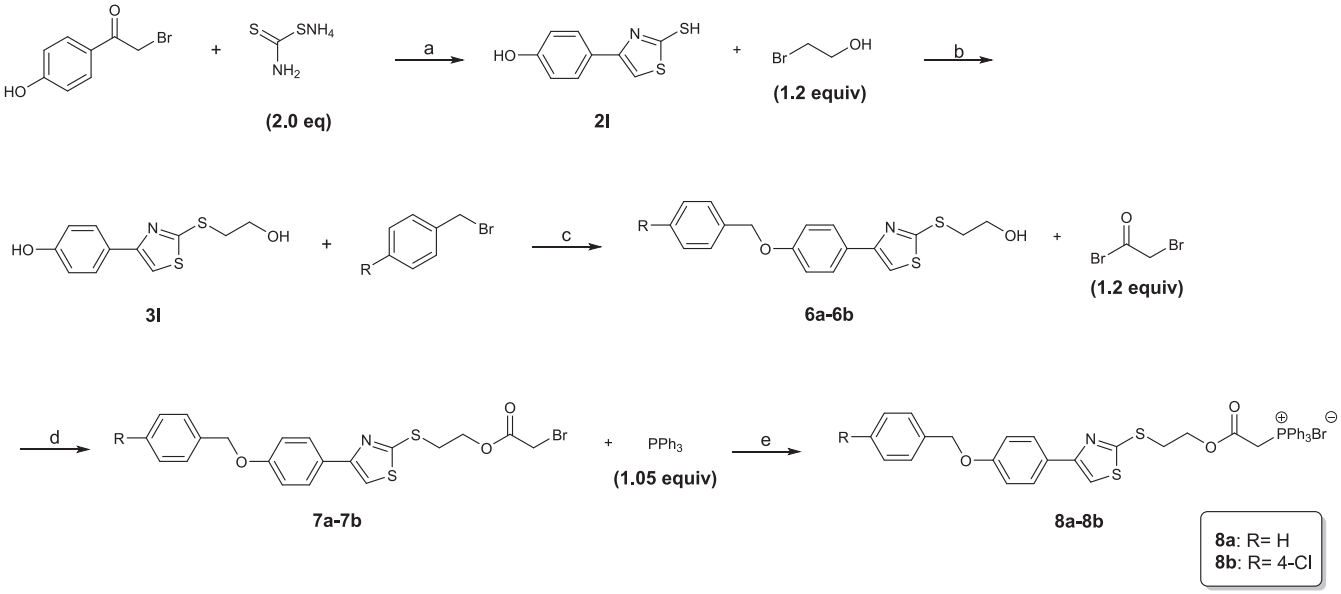

Scheme 2. Synthesis of **8a**-**8b**. Reaction conditions: a: EtOH, H_2O, 0 °C to 80 °C, 3 h. b: K_2CO_3 (1.2 equiv), acetone, rt, 4 h. c: K_2CO_3 (1.2 equiv), CH_3CN, 80 °C, 16 h. d: THF, 0 °C to rt, 2 h. e: CH_3CN, rt, overnight.

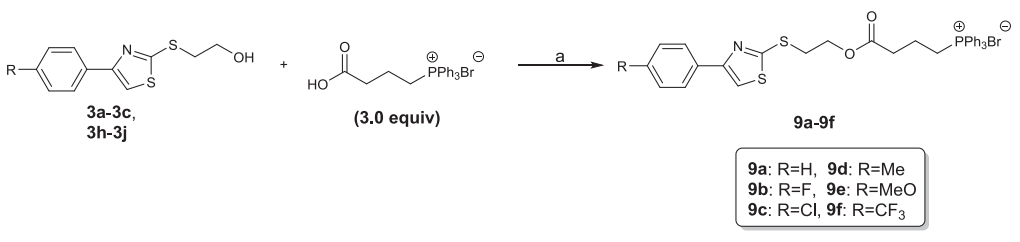

Scheme 3. Synthesis of **9a**-**9f**. Reaction conditions: a: EDCI (3.0 equiv), DMAP (1.0 equiv), DCM, rt, 6 h.

(**9a**-**9f**) was not improved, in contrast to series **5**.

On the other hand, longer carbon chain between 4-aryl-1,3-thiazole ring and ester group positively affected the potency. Compounds **12a**-**12c** showed good activities against four tested cancer cell lines compared to **5c**. Notably, compound **12a** displayed better activity than **12b** and **12c** in general, suggesting that further increasing the length between 4-aryl-1,3-thiazole ring and ester group would not lead to a stronger activity on anti-proliferation. The structure–activity

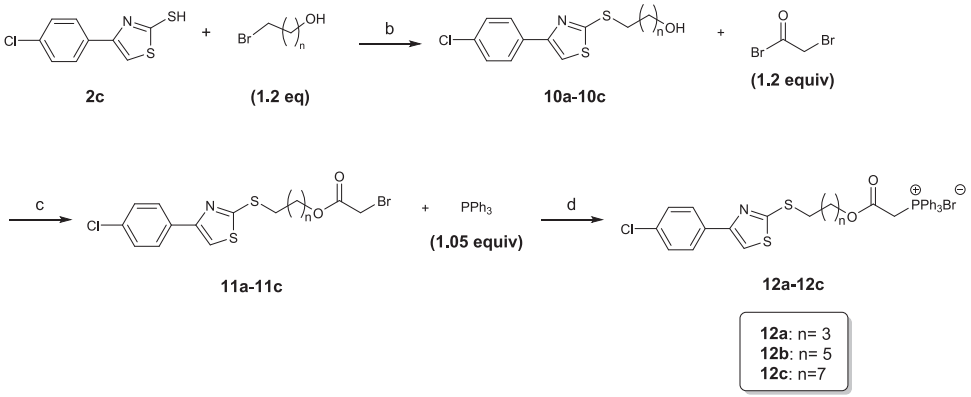

Scheme 4. Synthesis of **12a-12c**. Reaction conditions: a: K_2CO_3 (1.2 equiv), acetone, rt, 4 h. b: DCM, 0 °C to rt, 2 h. c: CH_3CN, rt, overnight.

Table 1
Cytotoxic effects of novel 4-Aryl-1,3-thiazole-TPP conjugates on cancer cell lines.

Compound	R	IC_{50} (μM)[a]			
		HeLa	MCF-7	PC-3	HCT-15
5a	H	29.36 ± 3.20	41.98 ± 2.23	>50	35.09 ± 2.36
5b	4-F	28.52 ± 2.24	>50	>50	44.76 ± 0.67
5c	4-Cl	15.45 ± 1.13	32.79 ± 1.71	31.24 ± 1.73	26.97 ± 2.08
5d	3-Cl	15.73 ± 0.62	>50	23.74 ± 2.25	18.53 ± 1.28
5e	4-Br	18.66 ± 1.05	45.50 ± 0.84	27.83 ± 1.43	19.49 ± 2.24
5f	3-Br	25.51 ± 0.42	31.78 ± 0.70	33.57 ± 2.29	19.49 ± 0.73
5g	4-Me	24.76 ± 2.06	32.49 ± 1.51	20.65 ± 1.63	21.02 ± 1.11
5h	4-MeO	33.45 ± 0.45	>50	>50	>50
5i	4-CF_3	22.18 ± 1.75	20.53 ± 2.48	22.55 ± 1.72	20.25 ± 0.90
5j	4-CN	>50	>50	>50	>50
5k	4-NO_2	>50	>50	>50	>50
8a	H	>50	>50	18.07 ± 1.79	10.19 ± 0.98
8b	Cl	>50	>50	32.53 ± 1.80	20.19 ± 1.21
9a	H	>50	>50	>50	41.36 ± 0.31
9b	F	33.22 ± 0.29	20.49 ± 0.58	30.98 ± 1.49	29.64 ± 0.44
9c	Cl	31.57 ± 1.18	22.40 ± 0.85	23.19 ± 1.01	17.37 ± 0.71
9d	Me	>50	35.14 ± 0.50	35.71 ± 0.42	40.92 ± 0.64
9e	MeO	>50	32.98 ± 0.72	32.22 ± 0.50	48.23 ± 0.77
9f	CF_3	20.78 ± 0.70	19.10 ± 0.84	14.09 ± 0.53	12.53 ± 0.56
12a	Cl, n = 3	8.83 ± 0.81	15.81 ± 1.04	10.07 ± 0.94	7.84 ± 0.85
12b	Cl, n = 5	9.23 ± 0.14	23.09 ± 0.62	11.67 ± 0.86	9.95 ± 0.13
12c	Cl, n = 7	18.18 ± 0.81	21.64 ± 1.23	9.76 ± 0.59	10.25 ± 0.63
Dox[b]		1.15 ± 0.30	14.71 ± 0.37	>50	20.65 ± 0.92
Dasatinib[b]		52.98 ± 0.82	36.03 ± 0.66	32.17 ± 0.62	41.24 ± 0.47
CCCP[b]		>50	>50	>50	>50

[a] IC_{50} values are presented as the mean ± SD (standard error of the mean) from 3 independent experiments. [b] Doxorubicin, Dasatinib and CCCP were used as a positive control.

relationship (SAR) of our final compounds is summarized in Fig. 3. Besides, **12a-12c** were less toxic toward BEAS-2B cells (Table 2). Given the most potency against HeLa cells, **12a** was chosen for further investigation.

2.3. Colony formation assay

The colony formation assay was performed to verify the ability of compound **12a** to repress proliferation. As shown in Fig. 4, the numbers of HeLa cell colonies decreased distinctly with increasing concentrations of compound **12a** (0, 3.125, 6.25, 12.5 μM). It can be concluded that compound **12a** could inhibit the proliferation of HeLa cells in a dose-dependent manner.

2.4. Determination of mitochondrial membrane potential (MMP)

Mitochondria are polarized because of the negative electric potential differences across the inner membrane. Appropriate mitochondrial polarization is important for cellular energy metabolism. In contrast, depolarization is an indicator of mitochondrial dysfunction. The mitochondrial membrane potential (MMP) was detected using the fluorescent probe JC-1, a lipophilic cationic dye. When the MMP is low, the dye exists as monomer emitting green fluorescence (λ_{ex} = 514 nm, λ_{em} = 529 nm). As the MMP is high, there are more dyes accumulating in the mitochondria forming aggregates emitting red fluorescence (λ_{ex} = 585 nm, λ_{em} = 590 nm). The ratio of red/green fluorescence was used for evaluating the variation of MMP. As shown in Fig. 5A and B, 12a induced the depletion of MMP dose-dependently. After the treatment with increasing concentration of **12a** (0, 2.5, 5.0 and 10 μM) for 24 h, the MMP of HeLa cells were reduced to 78 %, 72 % and 40 % of the control group respectively, compared to the blank group. Carbonyl cyanide *m*-chlorophenylhydrazine (CCCP), a protonophore, was used as the positive control.

2.5. Measurement of intracellular reactive oxygen species (ROS)

Intracellular reactive oxygen species (ROS) are unavoidable byproducts of mitochondrial oxidative phosphorylation [34]. Low levels of ROS function as signaling molecules to stimulate survival and proliferation pathways, whereas high levels of ROS cause oxidative stress leading to cell death and apoptosis [35]. Recently, generation of cytotoxic oxidative stress has emerged as an effective strategy for cancer therapy [36].

To find out whether **12a** induced higher levels of ROS accumulation in the treated HeLa cells, DCFH-DA (2′,7′-dichlorofluorescein diacetate) fluorescent probe was used. DCFH-DA is hydrolyzed to DCFH by esterase after passing through the cell membrane of live cells. DCFH is oxidized to highly fluorescent DCF (dichlorofluorescein, λ_{ex} = 488 nm, λ_{em} = 525

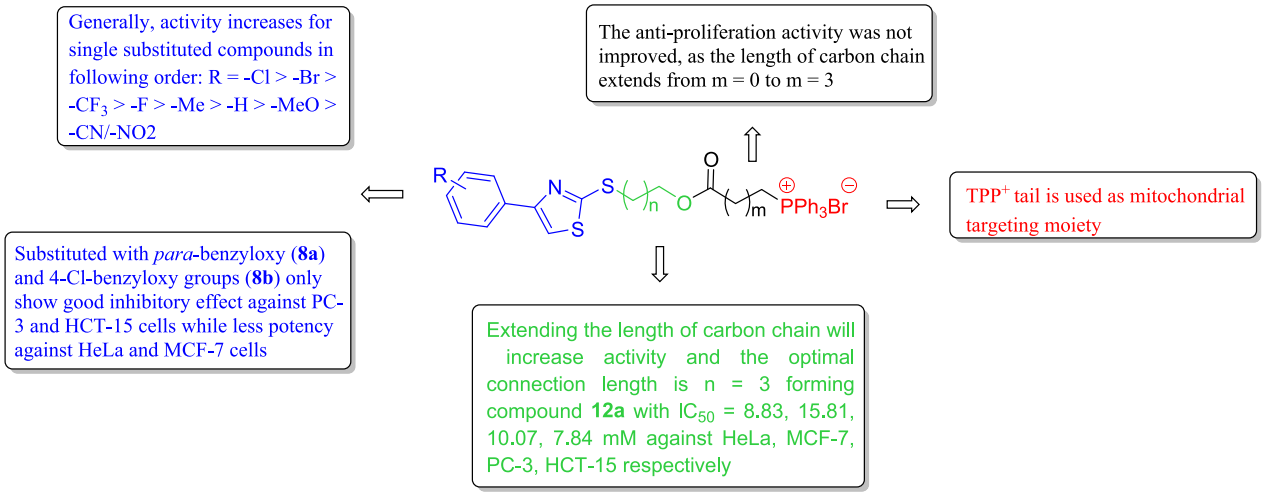

Fig. 3. Structrue-activity relationship for compounds **5a-5k, 8a-8b, 9a-9f** and **12-12c**.

Table 2
Cytotoxic Effects of Compound 12a-12 on BEAS-2B cells.

Compound	IC_{50} (μM)[a]
12a	16.74 ± 1.19
12b	26.70 ± 1.04
12c	21.32 ± 0.76

[a] IC_{50} values are presented as the mean ± SD (standard error of the mean) from 3 independent experiments.

nm) in the presence of ROS [37]. The intensity of green fluorescence produced by DCF indicates ROS level. As shown in Fig. 6A and 6B, treating with compound **12a** could remarkably promote ROS content compared with the control group (treated with DMSO). Different concentrations of **12a** (5.0 μM, 7.5 μM and 10.0 μM) induced 1.25-fold, 1.32-fold and 1.46-fold increase in ROS level, respectively.

2.6. Apoptosis analysis by flow cytometry assay

To explore if the cytotoxicity of **12a** is attributed to its induction of apoptosis, the Annexin V-FITC/PI dual staining was performed and analyzed by flow cytometry. As shown in Fig. 7, significant apoptotic effects were observed for **12a** in HeLa cells after 24 h treatment. The percentages of apoptosis for HeLa cells treated with **12a** at 5.0, 7.5, 10.0 μM for 24 h were 5.8 %, 9.8 % and 16.4 %, respectively, in a dose-dependent manner. These results suggested that the cytotoxicity of **12a** is mainly due to the induction of cell apoptosis.

2.7. Cell cycle analysis

Other than inducing apoptosis, we further investigated whether **12a** caused any cell cycle arrest on HeLa cells. The cell cycle phase distribution of HeLa cells treated with **12a** was analyzed by flow cytometry after propidium iodide staining. As shown in Fig. 8A-B, the distribution of G1 significantly increased after treating with **12a** with concentration range from 0-10 μM. The percentage of cells in G1 phase increased from 61.43 % to 85.97 %. Meanwhile, the ratio of cells in S and G2 phase slightly declined. These results indicated that **12a** induced G0/G1 cell cycle arrest in HeLa cells.

2.8. Mitochondrial bioenergetics assay

Oxidative phosphorylation (OXPHOS) and glycolysis are two main pathways of cellular ATP production in mammalian cells. OXPHOS consumes O_2, driving the oxygen consumption rate (OCR); hence OCR measurement can directly reflect the mitochondrial respiratory activity. Both glycolysis and OXPHOS can contribute to the acidification of the assay medium. The sum of these reactions is the primary driver of changes in extracellular acidification rate (ECAR). To investigate the direct effect of compound **12a** on cellular metabolism, we measured the oxygen consumption rate (OCR) and extracellular acidification rate (ECAR) of HeLa cells to determine mitochondrial respiration and glycolysis, respectively. An acute injection of **12a** at 10 μM was applied to all tests. The changes of OCR and ECAR values were monitored in real-time via a Seahorse XFp analyzer. As illustrated in Fig. 9A, compound **12a** caused a significant decrease in the OCR of HeLa cells. Compared with the blank group, the presence of **12a** quickly resulted in a decrease

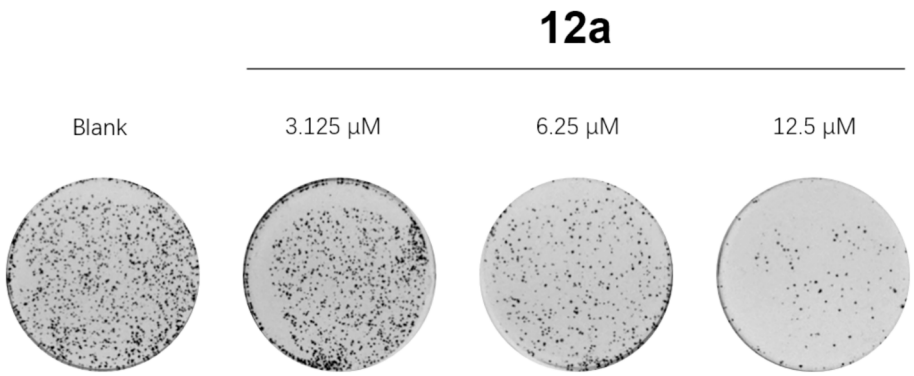

Fig. 4. Effects of compound 11a on colony formation assay. HeLa cells were treated with indicated concentrations of compound **12a** for 12 days.

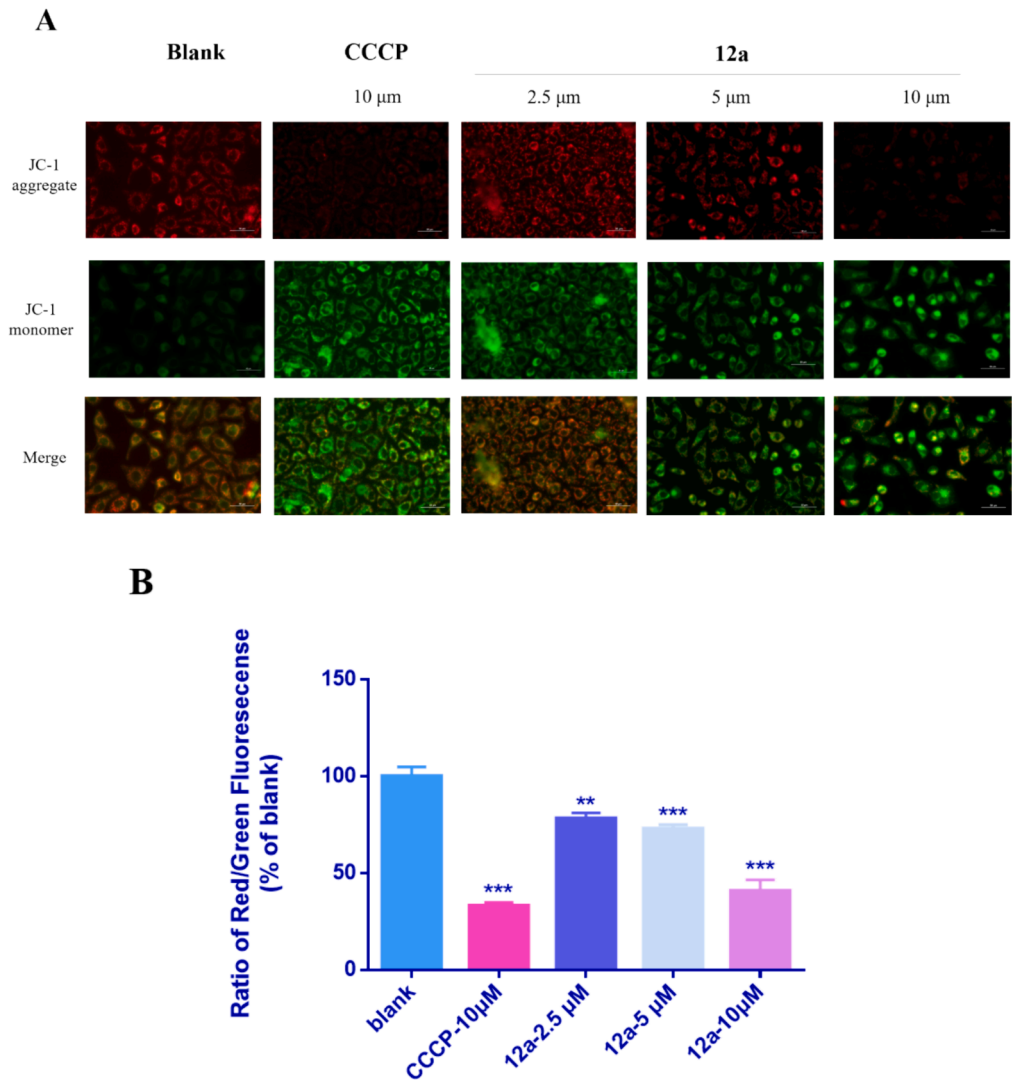

Fig. 5. Effects of **CCCP** and **12a** on Decreasing Mitochondrial Membrane Potential. (A) Images observed by fluorescence microscope. (B) Ratio of red fluorescence and green fluorescence. The values are presented as mean ± SD (n = 3). **P < 0.01, ***P < 0.001, ****P < 0.0001 vs. control group. (For interpretation of the references to colour in this figure legend, the reader is referred to the web version of this article.)

in maximal respiration and ATP production, as well as an increase in proton leak (Fig. 9B). Notably, a slightly elevated OCR was observed after addition of oligomycin, suggesting a mild uncoupling effect of **12a** [38,39]. These results were indicative of a severe mitochondrial impairment. In addition, the injection of **12a** induced a rapid elevation of glycolysis, shown in Fig. 9C. These findings suggest a metabolic shift from OXPHOS to glycolysis, which may be an adaptive response made by cells to compensate the mitochondrial ATP loss. Consistent with the ECAR data, this compensational response helped maintain total ATP production rate despite mitochondrial ATP production rate being sharply repressed (Fig. 9D).

2.9. Effect of *12a* on UCP-1 expression

Mitochondrial uncoupling is a process that leads to protons influx across the mitochondrial inner membrane independent of ATP synthase and uncouples nutrient oxidation from ATP production [40]. The energy dissipates as protons re-enter matrix without passing through ATP synthase. It can be easily understood that depletion of cellular ATP cellular caused by mitochondrial uncoupling will trigger responses to the stress [41].

In recent years, small molecules mitochondrial uncouplers have been developed for treating metabolic diseases [42–44] and cancers [39,45–48]. Small molecules mitochondrial uncouplers are usually divided into two broad classes: protonophores and non-protonophores [49,50]. Protonophore uncouples are lipophilic weak acids that can penetrate membranes such as 2,4-dinitrophenol (DNP), carbonyl cyanide *p*-(trifluoromethoxy)phenyl hydrazone (FCCP), carbonyl cyanide *m*-chlorophenyl hydrazine (CCCP) and BAM15 [51]. Non-protonophore uncouplers de-couple mitochondrial respiratory through other mechanisms such as a PPARγagonist [52] and uncoupling protein 1 (UCP1) activator [53]. UCP1 is a protein which is expressed in the inner membrane of mitochondria and functions to uncouple mitochondrial fatty acid oxidation from the production of ATP [54]. It is also reported that UCP1 can inhibit tumor progression by initiating autophagy, mitophagy and pyroptosis [55,56], along with snail-mediated repression of fructose-bisphosphatase 1(FBP1) [57]. Since compound **12a** might not function as a protonophore according to its chemical structure, one possible mechanism by which compound **12a** directly or indirectly uncouple mitochondrial respiration is regulating the expression of UCP1

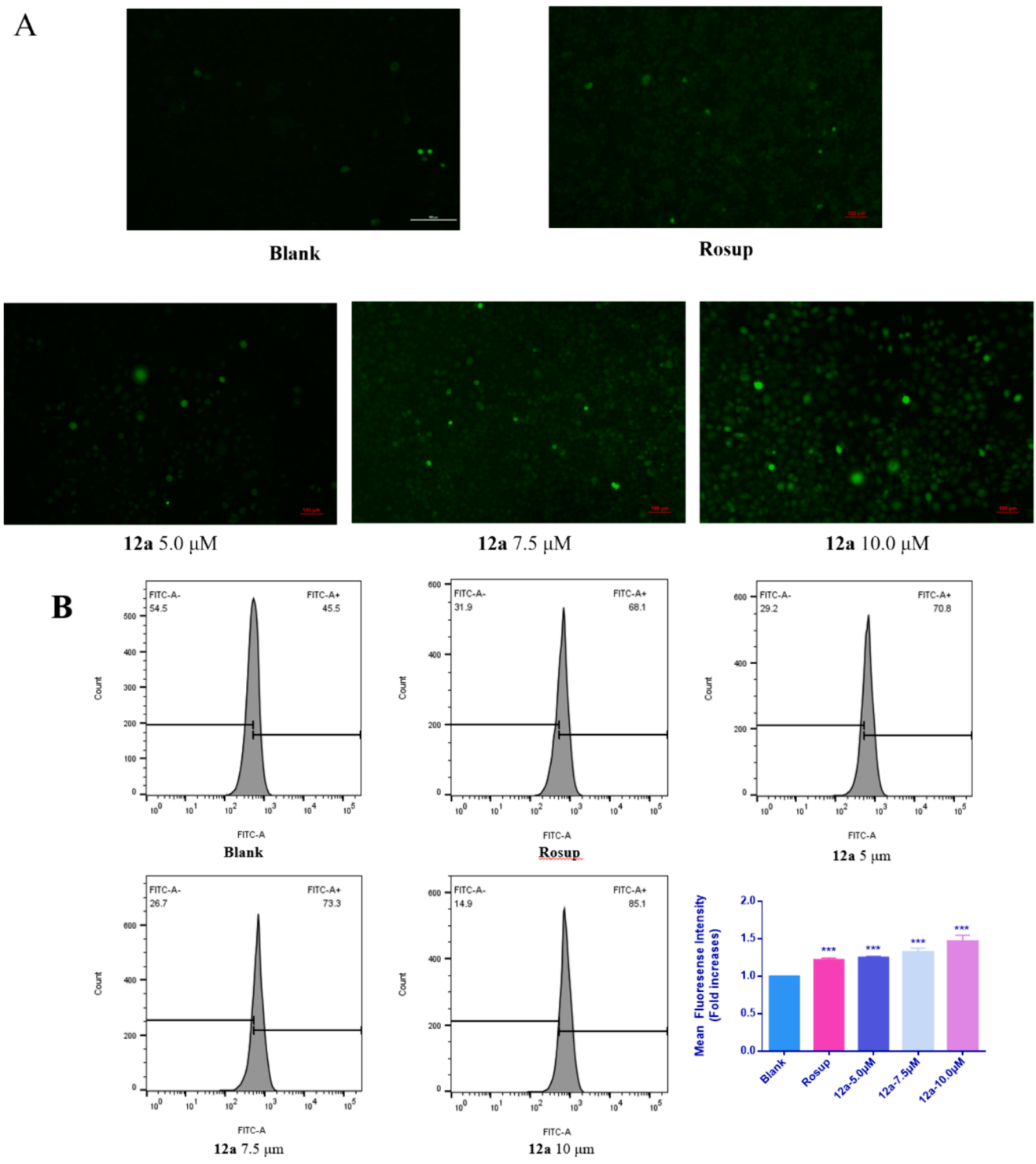

Fig. 6. Effects on intracellular ROS production of HeLa cells treated with **12a** at indicating concentrations for 24 h. A. Fluorescence microscopy images. B. Data analyzed by flow cytometry. **P < 0.01, ***P < 0.001, ****P < 0.0001 vs. blank group.

[53]. To elucidate the mechanism of energy expenditure elevation by treating HeLa cells with compound **12a**, we assessed the expression levels of UCP1 by western blot. CCCP was used as positive control. As illustrate in Fig. 10, the UCP1 expression level was upregulated after administrated with **12a** (10 μM) for 2 h. These results imply that the mitochondrial uncoupling effect of **12a** is associated with upregulation of UCP1.

3. Conclusions

In summary, a novel series of 4-aryl-1, 3-thiazole-TPP conjugates was successfully designed and synthesized and their anti-proliferative activities were evaluated. The results of CCK-8 assay demonstrate that linker length and structure significantly impact on the cytotoxic activities of these compounds. Specifically, while extending the linker length between 4-aryl-1,3-thiazole ring and ester group from 2 to 4, 6, and 8 carbon atoms, it significantly enhances the activities, further increasing

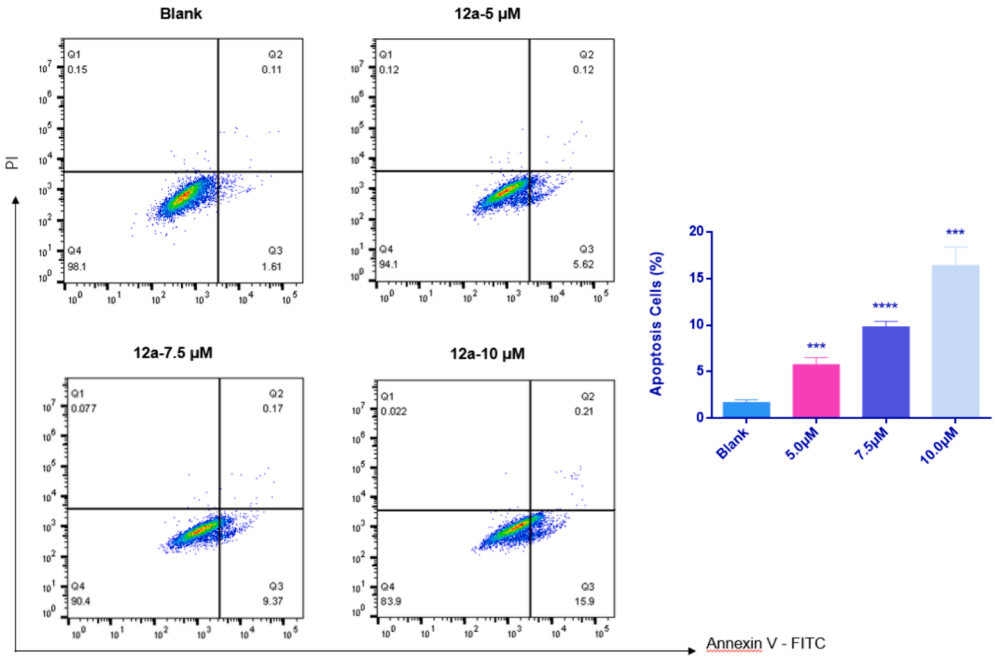

Fig. 7. Apoptotic effects of **12a** on HeLa cells. After treatment with **12a** at indicated concentration for 24 h, HeLa cells were stained with annexin V-FITC/PI and analyzed by flow cytometry. The percentages of apoptosis are presented as mean ± SD (n = 3). **P < 0.01, ***P < 0.001, ****P < 0.0001 vs. control group.

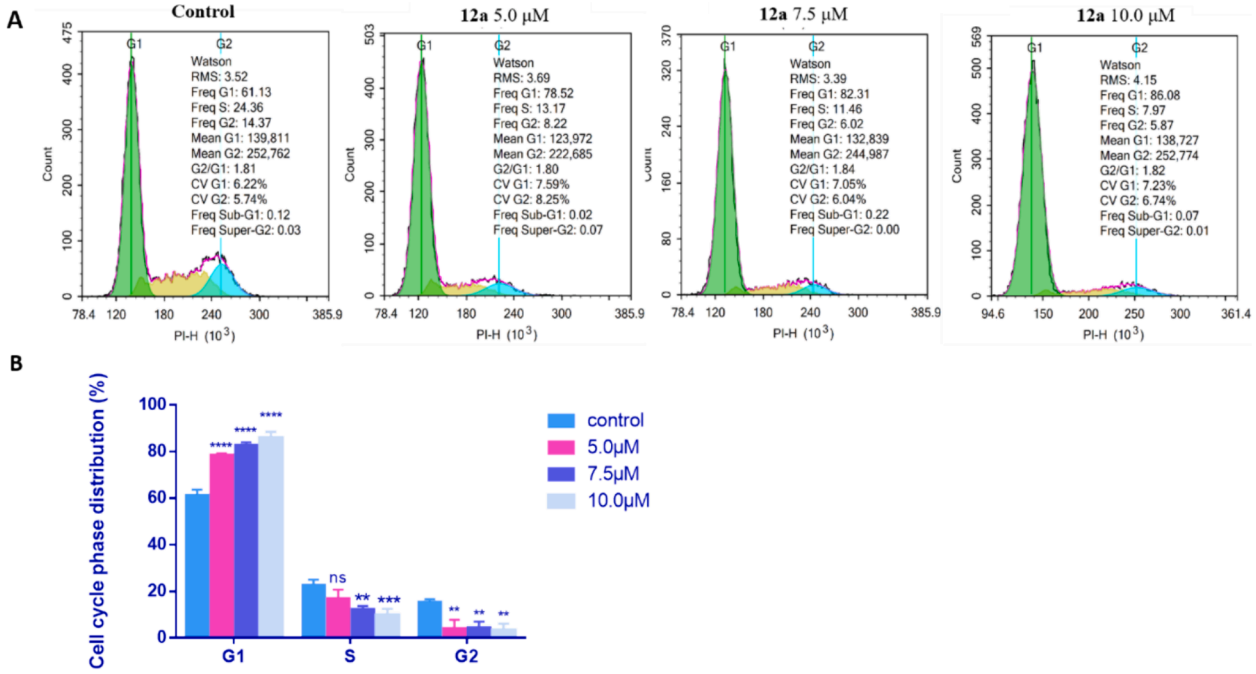

Fig. 8. Effects of **12a** on cell cycle arrest in HeLa cells. Cells were treated with different concentrations of **12a** (5, 7.5 and 10 μM) for 24 h, which were then stained with PI to analyze the DNA content by flow cytometry. A. Representative flow cytometry profiles. B. Percentage of HeLa cells in different phases of the cell cycle. The results are presented as mean ± SD (n = 3). **P < 0.01, ***P < 0.001, ****P < 0.0001 vs. control group.

the length between ester group and TPP^+ does not result in stronger anti-proliferative effects. Among all the compounds, **12a** displays most potent activity, effectively inhibiting the proliferation of HeLa cells with an IC_{50} value of 8.83 μM. The membrane potential of HeLa cells were reduced to 78 %, 72 % and 40 % of blank group respectively after the treatment with different concentration of **12a** (2.5, 5.0 and 10 μM). **12a** (5.0 μM, 7.5 μM and 10.0 μM) also induced 1.25-fold, 1.32-fold and 1.46-fold increase in ROS level. **12a** ultimately induces apoptosis in HeLa cells. The percentages of apoptosis for HeLa cells treated with **12a** at 5.0, 7.5, 10.0 μM were 5.8 %, 9.8 % and 16.4 %, in a dose-dependent manner. Furthermore, flow cytometry analysis indicated **12a** arrested cell cycle at G0/G1 phase. The percentage of cells in G1 phase significantly increased from 61.43 % to 85.97 % after the treatment of **12a** with different concentrations. Notably, **12a** altered the metabolism of HeLa cells by inhibiting OXPHOS after acute injection. Moreover, a mild mitochondrial uncoupling effect is observed, possibly attributed to the upregulation of UCP1 expression. These findings provide valuable insights for *in vivo* animal studies and further development of potential

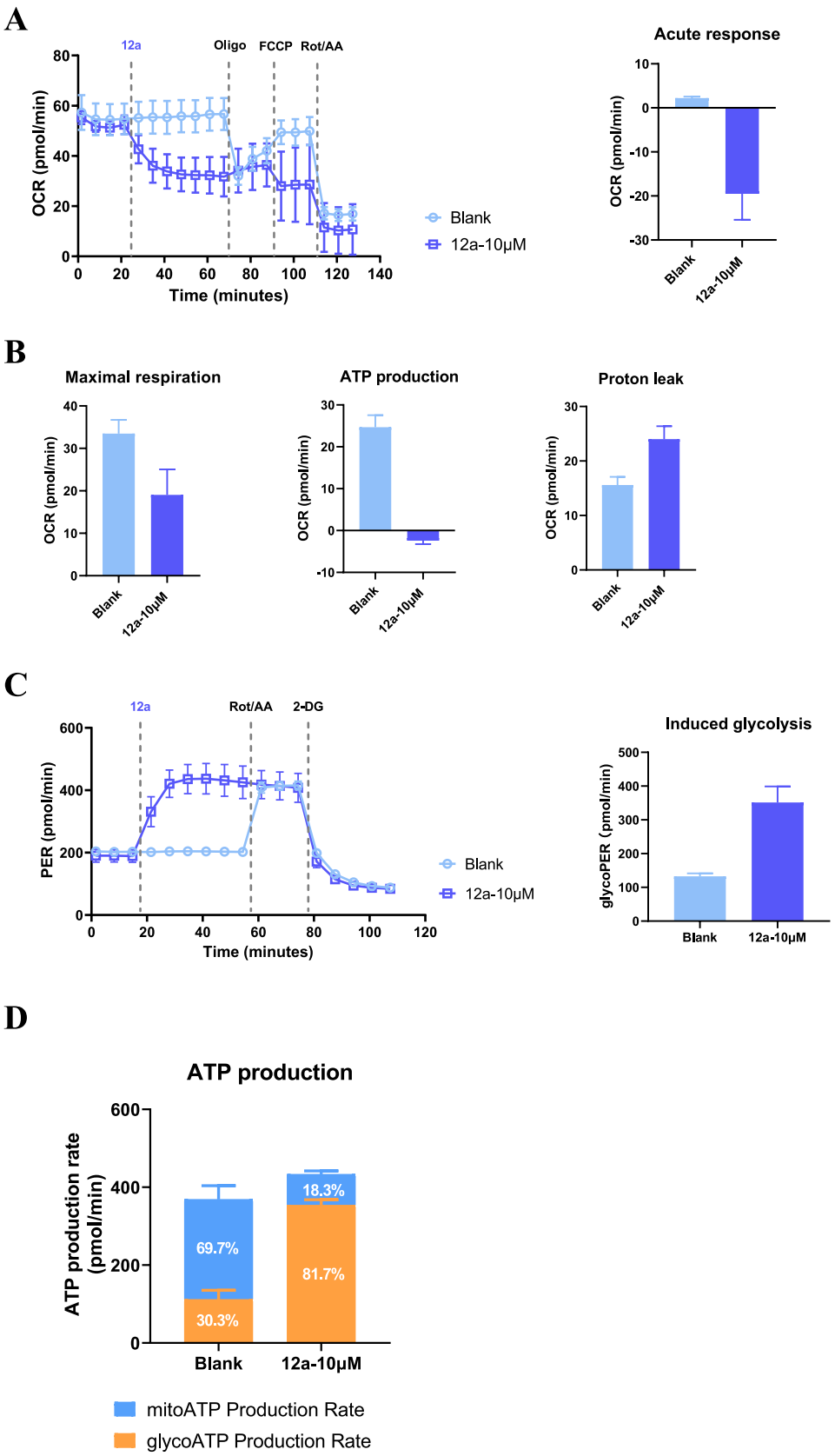

Fig. 9. Effects of **12a** on cellular metabolism of HeLa. (A) Induced mito stress test. (B) Maximal respiration, ATP production. Proton leak. Values are calculated with OCR and presented as mean ± SD (n = 3). (C) Induced glycolytic rate assay. ECAR transformed into a rate that reflects the number of protons extruded over time, proton efflux rate PER. (D) Induced real-time ATP rate assay.

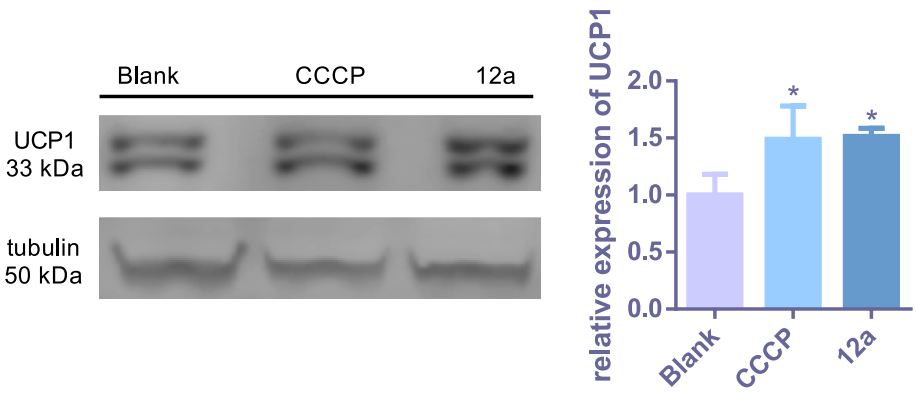

Fig. 10. Effects of **12a** (10 μM) on UCP1 expression in HeLa cells. Western blotting images and quantification data.

anticancer agents targeting mitochondrial functions.

4. Experimental

4.1. Reagents and general methods

All the chemicals were obtained from commercial suppliers, without further purification. The targeted compounds were isolated using column chromatography on silica gel (200–300 mesh, Huanghai, China). All tested cells were purchased from Cell Bank of the Shanghai Institute of Biochemistry and Cell Biology (Chinese Academy of Sciences, Shanghai, China). Cell culture media (DMEM, RPI-1640 and F12) were purchased from Biosharp. Fetal bovine serum (FBS) was purchased from Biological Industries. Penicillin/streptomycin were purchased from HyClone. Cell Counting Kit-8 (CCK-8) was purchased from GLPBIO. JC-1 and DCFH-DA Kit were purchased from Beyotime (China). Annexin V-FITC/PI apoptotic detection kit was ordered from Elabscience (China). RIPA buffer, protease inhibitor (PMSF) and BCA Protein Assay Kit were purchased from Beyotime (China). 4–20 % Bis-Tris gel (SurePAGE) was purchased from GenScript (USA). Primary antibodies: Beta tubulin (AB0039) was ordered from Abways (China), UCP-1 (23673-AP) was ordered from Proteintech (China). Secondary antibodies: Goat-mouse IRDye 800 (Licor), Goat-Rabbit 680 (Licor).

NMR (^{1}H, ^{13}C and ^{31}P) spectra were recorded on Agilent 400 MHz or Bruker Avance 400 NMR spectrometers. Chemical shifts were expressed in parts per million (ppm). Coupling constants were in units of Hertz (Hz). Splitting patterns describe apparent multiplicities were designated as s (singlet), d (doublet), t (triplet), q (quartet), m (multiplet) and br (broad). The NMR data was analyzed by MestReNova software. High-resolution mass spectra (HRMS) was acquired on an Agilent 6200 TOF LC/MS system, UV detector (220 and 254 nm).

4.2. Chemical Synthesis

4.2.1. General procedure for the synthesis of 2a-2l [33,58]

Ammonium dithiocarbamate (20 mmol) was dissolved in a mixture of ethanol (20 mL) and water (20 mL). 2-bromo-1-phenylethanone (**1a,** 10 mmol) was added in portion under ice bath and the mixture was refluxed for 5 h. 30 mL water was then added to the mixture in order to precipitate product. The solid were obtained by filter and recrystallized by ethanol. Yields of **2a**-**2l** were determined by recrystallization.

*4.2.1.1. 4-phenylthiazole-2-thiol (**2a**).* White solid (1.02 g, 53 % yield). ^{1}H NMR (400 MHz, $CDCl_3$) δ 11.85 (s, 1H), 7.54 (dd, J = 9.4, 2.8 Hz, 2H), 7.45 (td, J = 8.8, 4.6 Hz, 3H), 6.69 (s, 1H). ^{13}C NMR (101 MHz, $CDCl_3$) δ 190.0, 142.3, 129.9, 129.4, 128.4, 126.1, 108.5.

*4.2.1.2. 4-(4-fluorophenyl)thiazole-2-thiol (**2b**).* White solid (0.99 g, 47 % yield). ^{1}H NMR (400 MHz, $CDCl_3$) δ 11.79 (s, 1H), 7.53 (dd, J = 8.8, 5.1 Hz, 2H), 7.16 (t, J = 8.5 Hz, 2H), 6.64 (s, 1H). ^{13}C NMR (101 MHz, $CDCl_3$) δ 190.1, 164.8, 162.3, 141.2, 128.1 (d, J = 8.5 Hz), 116.7 (d, J = 22.2 Hz), 108.3 (d, J = 1.4 Hz).

*4.2.1.3. 4-(4-chlorophenyl)thiazole-2-thiol (**2c**).* White solid (1.16 g, 51 % yield). ^{1}H NMR (400 MHz, DMSO-d_6) δ 13.67 (s, 1H), 7.76 (d, J = 8.6 Hz, 2H), 7.51 (d, J = 8.7 Hz, 2H), 7.35 (s, 1H). ^{13}C NMR (101 MHz, DMSO-d_6) δ 189.6, 140.4, 133.7, 128.9, 127.6, 127.3, 110.0.

*4.2.1.4. 4-(3-chlorophenyl)thiazole-2-thiol (**2d**).* White solid (1.39 g, 61 % yield). ^{1}H NMR (400 MHz, DMSO-d_6) δ 13.69 (s, 1H), 7.89 (dd, J = 2.1, 1.5 Hz, 1H), 7.74–7.71 (m, 1H), 7.48–7.44 (m, 3H). ^{13}C NMR (101 MHz, DMSO-d_6) δ 189.6, 140.0, 133.7, 130.7, 130.3, 128.8, 125.5, 124.4, 110.8.

*4.2.1.5. 4-(4-bromophenyl)thiazole-2-thiol (**2e**).* White solid (1.64 g, 60 % yield). ^{1}H NMR (400 MHz, DMSO-d_6) δ 13.67 (s, 1H), 7.70 (d, J = 8.7 Hz, 2H), 7.64 (d, J = 8.7 Hz, 2H), 7.36 (s, 1H). ^{13}C NMR (101 MHz, DMSO-d_6) δ 189.7, 140.5, 131.8, 130.5, 127.8, 122.4, 110.1.

*4.2.1.6. 4-(3-bromophenyl)thiazole-2-thiol (**2f**).* White solid (1.77 g, 65 % yield). ^{1}H NMR (400 MHz, DMSO-d_6) δ 13.69 (s, 1H), 8.03 (t, J = 1.8 Hz, 1H), 7.77 (ddd, J = 7.9, 1.7, 0.9 Hz, 1H), 7.60 (ddd, J = 8.0, 1.9, 0.9 Hz, 1H), 7.47 (s, 1H), 7.41 (t, J = 7.9 Hz, 1H). ^{13}C NMR (101 MHz, DMSO-d_6) δ 189.6, 139.8, 131.7, 130.9, 130.5, 128.3, 124.7, 122.2, 110.7.

*4.2.1.7. 4-(p-tolyl)thiazole-2-thiol (**2g**).* White solid (0.85 g, 41 % yield). ^{1}H NMR (400 MHz, $CDCl_3$) δ 12.04 (s, 1H), 7.43 (d, J = 8.2 Hz, 2H), 7.26 (d, J = 7.3 Hz, 2H), 6.64 (s, 1H), 2.38 (s, 3H). ^{13}C NMR (101 MHz, $CDCl_3$) δ 189.7, 142.5, 140.2, 130.1, 126.0, 125.6, 107.6, 21.4.

*4.2.1.8. 4-(4-methoxyphenyl)thiazole-2-thiol (**2h**).* White solid (0.94 g, 42 % yield). ^{1}H NMR (400 MHz, DMSO-d_6) δ 13.54 (s, 1H), 7.69 (d, J = 8.9 Hz, 2H), 7.15 (s, 1H), 7.00 (d, J = 8.9 Hz, 2H), 3.79 (s, 3H). ^{13}C NMR (101 MHz, DMSO-d_6) δ 189.3, 159.8, 141.5, 127.3, 121.1, 114.2, 107.0, 55.2.

*4.2.1.9. 4-(4-(trifluoromethyl)phenyl)thiazole-2-thiol (**2i**).* White solid (1.23 g, 47 % yield). ^{1}H NMR (400 MHz, $CDCl_3$) δ 12.19 (s, 1H), 7.74 (d, J = 8.5 Hz, 2H), 7.68 (d, J = 8.3 Hz, 2H), 6.84 (s, 1H). ^{13}C NMR (101 MHz, $CDCl_3$) δ 190.3, 140.9, 132.0, 131.8–131.4 (m), 126.7–126.3 (m), 125.1, 122.4, 110.5.

*4.2.1.10. 4-(2-mercaptothiazol-4-yl)benzonitrile (**2j**).* White solid (1.28 g, 59 % yield). ^{1}H NMR (400 MHz, DMSO-d_6) δ 13.80 (s, 1H), 7.94 (d, J = 2.6 Hz, 4H), 7.60 (s, 1H). ^{13}C NMR (101 MHz, DMSO-d_6) δ 189.8, 139.8, 132.8, 132.4, 126.4, 118.3, 112.7, 111.2.

*4.2.1.11. 4-(4-nitrophenyl)thiazole-2-thiol (**2k**).* White solid (1.41 g, 59 % yield). ^{1}H NMR (400 MHz, DMSO-d_6) δ 13.90 (s, 1H), 8.29 (d, J = 8.7 Hz, 2H), 8.03 (d, J = 8.7 Hz, 2H), 7.67 (s, 1H). ^{13}C NMR (101 MHz, DMSO-d_6) δ 189.9, 147.1, 139.5, 134.1, 126.8, 124.1, 113.6.

*4.2.1.12. 4-(2-mercaptothiazol-4-yl)phenol (**2l**).* White solid (0.85 g, 41 % yield). ^{1}H NMR (400 MHz, DMSO-d_6) δ 13.47 (s, 1H), 9.85 (s, 1H), 7.56 (d, J = 8.6 Hz, 2H), 7.04 (s, 1H), 6.81 (d, J = 8.7 Hz, 2H). ^{13}C NMR (101 MHz, DMSO-d_6) δ 189.3, 158.3, 141.9, 127.4, 119.7, 115.5, 106.2.

*4.2.2. General procedure for the synthesis of **3a**-**3l***

Thiazole-2-thiol (**2a**) (5 mmol), 2-bromo-ethanol (6 mmol) and potassium carbonate (6 mmol) were dissolved in acetone (20 mL) and stirred for 4 h. The solvent was removed under reduced pressure. The residue was purified by flash silica-gel column chromatography (PE/EA = 3/1, v/v). Yields of **3a**-**3l** were determined after column chromatograghy.

*4.2.2.1. 2-((4-phenylthiazol-2-yl)thio)ethan-1-ol (**3a**).* Colorless oil (0.81 g, 68 % yield). ^{1}H NMR (400 MHz, DMSO-d_6) δ 7.99 (s, 1H), 7.93 (d, J = 7.3 Hz, 2H), 7.44 (t, J = 7.6 Hz, 2H), 7.34 (t, J = 7.3 Hz, 1H), 5.15 (t, J = 5.3 Hz, 1H), 3.76 (dd, J = 11.7, 6.2 Hz, 2H), 3.38 (t, J = 6.4 Hz, 2H). ^{13}C NMR (100 MHz, DMSO-d_6) δ 164.4, 154.1, 133.6, 128.7, 128.1, 125.9, 113.9, 59.9, 36.6. HRMS (ESI), $C_{11}H_{11}NOS_2$ calcd for (M + H)$^+$ 238.0355, found 238.0349.

*4.2.2.2. 2-((4-(4-fluorophenyl)thiazol-2-yl)thio)ethan-1-ol (**3b**).* Colorless oil (0.76 g, 60 % yield). ^{1}H NMR (400 MHz, $CDCl_3$) δ 7.77 (dd, J = 8.9, 5.3 Hz, 2H), 7.27 (s, 1H), 7.08 (t, J = 8.7 Hz, 2H), 4.05–4.02 (m, 2H), 3.41–3.38 (m, 2H). ^{13}C NMR (100 MHz, $CDCl_3$) δ 165.2, 164.1, 161.6, 154.2, 129.9 (d, J = 3.0 Hz), 128.0 (d, J = 8.2 Hz), 115.9, 115.7, 112.9, 62.7, 37.6. HRMS (ESI), $C_{11}H_{10}FNOS_2$ calcd for (M + H)$^+$ 2560.0261, found 256.0262.

*4.2.2.3. 2-((4-(4-chlorophenyl)thiazol-2-yl)thio)ethan-1-ol (**3c**).* White solid (0.95 g, 70 % yield). ^{1}H NMR (400 MHz, $CDCl_3$) δ 7.73 (d, J = 8.7 Hz, 2H), 7.36 (d, J = 8.7 Hz, 2H), 7.33 (s, 1H), 4.22 (s, 1H), 4.06–4.02 (m, 2H), 3.43–3.40 (m, 2H). ^{13}C NMR (100 MHz, $CDCl_3$) δ 165.3, 154.1, 134.34 132.1, 129.1, 127.5, 113.6, 62.7, 37.6. HRMS (ESI), $C_{11}H_{10}ClNOS_2$ calcd for (M + H)$^+$ 271.9965, found 271.9961.

*4.2.2.4. 2-((4-(3-chlorophenyl)thiazol-2-yl)thio)ethan-1-ol (**3d**).* White solid (0.91 g, 67 % yield). ^{1}H NMR (400 MHz, $CDCl_3$) δ 7.79 (t, J = 1.8 Hz, 1H), 7.69 (dt, J = 7.5, 1.5 Hz, 1H), 7.37 (s, 1H), 7.34 (s, 1H), 7.31–7.28 (m, 1H), 4.06–4.03 (m, 2H), 3.43 (dd, J = 5.6, 4.7 Hz, 2H). ^{13}C NMR (100 MHz, $CDCl_3$) δ 165.4, 153.8, 135.3, 134.9, 130.2, 128.4, 126.3, 124.4, 114.2, 62.6, 37.6. HRMS (ESI), $C_{11}H_{10}ClNOS_2$ calcd for (M + H)$^+$ 271.9965, found 271.9953.

*4.2.2.5. 2-((4-(4-bromophenyl)thiazol-2-yl)thio)ethan-1-ol (**3e**).* White solid (1.19 g, 75 % yield). ^{1}H NMR (400 MHz, DMSO-d_6) δ 8.06 (s, 1H), 7.88 (d, J = 8.6 Hz, 2H), 7.63 (d, J = 8.6 Hz, 2H), 5.11 (s, 1H), 3.74 (t, J = 6.4 Hz, 2H), 3.37 (t, J = 6.4 Hz, 2H). ^{13}C NMR (100 MHz, DMSO-d_6) δ 164.9, 152.9, 132.8, 131.7, 127.9, 121.2, 114.7, 59.6, 36.6. HRMS (ESI), $C_{11}H_{10}BrNOS_2$ calcd for (M + H)$^+$ 315.9460, found 315.9461.

*4.2.2.6. 2-((4-(3-bromophenyl)thiazol-2-yl)thio)ethan-1-ol (**3f**).* White solid (1.13 g, 72 % yield). ^{1}H NMR (400 MHz, $CDCl_3$) δ 7.95 (t, J = 1.8 Hz, 1H), 7.75 (ddd, J = 7.8, 1.6, 1.0 Hz, 1H), 7.46 (ddd, J = 8.0, 1.9, 1.0 Hz, 1H), 7.37 (s, 1H), 7.28 (t, J = 7.5 Hz, 1H), 4.05 (d, J = 5.3 Hz, 2H), 3.90 (t, J = 5.3 Hz, 1H), 3.45–3.43 (m, 2H). ^{13}C NMR (100 MHz, $CDCl_3$) δ 165.40, 153.74, 135.67, 131.43, 130.52, 129.31, 124.92, 123.08, 114.28, 62.63, 37.70. HRMS (ESI), $C_{11}H_{10}BrNOS_2$ calcd for (M + H)$^+$ 315.9460, found 315.9461.

*4.2.2.7. 2-((4-(p-tolyl)thiazol-2-yl)thio)ethan-1-ol (**3g**).* Colorless oil (0.80 g, 64 % yield). ^{1}H NMR (400 MHz, $CDCl_3$) δ 7.70 (d, J = 7.9 Hz, 2H), 7.28 (s, 1H), 7.21 (d, J = 7.9 Hz, 2H), 4.57 (s, 1H), 4.05 (t, J = 5.2 Hz, 2H), 3.40 (t, J = 5.1 Hz, 2H), 2.37 (s, 3H). ^{13}C NMR (100 MHz, $CDCl_3$) δ 164.8, 155.4, 138.5, 130.9, 129.6, 126.2, 112.6, 63.0, 37.8, 21.4. HRMS (ESI), $C_{12}H_{13}NOS_2$ calcd for (M + H)$^+$ 252.0511, found 252.0504.

*4.2.2.8. 2-((4-(4-methoxyphenyl)thiazol-2-yl)thio)ethan-1-ol (**3h**).* White solid (0.87 g, 65 % yield). ^{1}H NMR (400 MHz, DMSO-d_6) δ 7.85 (d, J = 8.9 Hz, 2H), 7.82 (s, 1H), 6.99 (d, J = 8.9 Hz, 2H), 5.11 (t, J = 5.5 Hz, 1H), 3.79 (s, 3H), 3.74 (dd, J = 12.1, 6.3 Hz, 2H), 3.37–3.35 (m, 2H). ^{13}C NMR (100 MHz, DMSO-d_6) δ 164.1, 159.2, 154.1, 127.3, 126.5, 114.1, 111.9, 59.7, 55.2, 36.6. HRMS (ESI), $C_{12}H_{13}NO_2S_2$, calcd for (M + H)$^+$ 268.0460, found 268.0462.

*4.2.2.9. 2-((4-(4-(trifluoromethyl)phenyl)thiazol-2-yl)thio)ethan-1-ol (**3i**).* White solid (1.08 g, 71 % yield). ^{1}H NMR (400 MHz, $CDCl_3$) δ 7.91 (d, J = 8.1 Hz, 2H), 7.65 (d, J = 8.2 Hz, 2H), 7.45 (s, 1H), 4.05 (t, J = 5.3 Hz, 2H), 4.01 (s, 1H), 3.46–3.42 (m, 2H). ^{13}C NMR (100 MHz, $CDCl_3$) δ 165.8, 153.8, 136.9, 130.8, 130.5, 130.2, 129.8, 126.5, 125.9 (q, J = 3.8 Hz), 125.6, 122.9, 115.1, 62.6, 37.7. HRMS (ESI), $C_{12}H_{10}F_3NOS_2$ calcd for (M + H)$^+$ 306.0229, found 306.0227.

*4.2.2.10. 4-(2-((2-hydroxyethyl)thio)thiazol-4-yl)benzonitrile (**3j**).* White solid (0.90 g, 69 % yield). ^{1}H NMR (400 MHz, DMSO-d_6) δ 8.28 (s, 1H), 8.11 (d, J = 8.6 Hz, 2H), 7.90 (d, J = 8.6 Hz, 2H), 5.12 (s, 1H), 3.75 (t, J = 6.0 Hz, 2H), 3.39 (t, J = 6.4 Hz, 2H). ^{13}C NMR (100 MHz, DMSO-d_6) δ 165.5, 152.2, 137.6, 132.8, 126.5, 118.8, 117.3, 110.3, 59.6, 36.6. HRMS (ESI), $C_{12}H_{10}N_2OS_2$ calcd for (M + H)$^+$ 263.0307, found 263.0311.

*4.2.2.11. 2-((4-(4-nitrophenyl)thiazol-2-yl)thio)ethan-1-ol (**3k**).* Yellow solid (0.76 g, 54 % yield). ^{1}H NMR (400 MHz, $CDCl_3$) δ 8.26 (d, J = 8.9 Hz, 2H), 7.98 (d, J = 8.8 Hz, 2H), 7.57 (s, 1H), 4.06 (d, J = 4.2 Hz, 2H), 3.65 (s, 1H), 3.47 (t, J = 5.4 Hz, 2H). ^{13}C NMR (100 MHz, $CDCl_3$) δ 166.4, 152.9, 147.5, 139.5, 126.9, 124.4, 116.6, 62.5, 37.6. HRMS (ESI), $C_{11}H_{10}N_2O_3S_2$ calcd for (M + H)$^+$ 283.0206, found 283.0203.

*4.2.2.12. 4-(2-((2-hydroxyethyl)thio)thiazol-4-yl)phenol (**3l**).* White solid (0.86 g, 68 % yield). ^{1}H NMR (400 MHz, DMSO-d_6) δ 9.64 (s, 1H), 7.74 (d, J = 8.6 Hz, 2H), 7.71 (s, 1H), 6.82 (d, J = 8.6 Hz, 2H), 5.12 (s, 1H), 3.74 (t, J = 6.2 Hz, 2H), 3.34 (t, J = 6.5 Hz, 2H). ^{13}C NMR (100 MHz, DMSO-d_6) δ 163.8, 157.5, 154.5, 127.4, 125.0, 115.5, 110.9, 59.7, 36.6. HRMS (ESI), $C_{11}H_{11}NO_2S_2$ calcd for (M + H)$^+$ 254.0304, found 254.0304.

*4.2.3. General procedure for the synthesis of **4a**-**4k***

To a stirred solution of compound **3a** (10 mmol) in 20 mL DCM under ice bath was added bromoacetyl bromide (12 mmol). The reaction mixture was stirred for 2 h under room temperature and washed by saturated aqueous $NaHCO_3$ and brine, dried over by anhydrous Na_2SO_4 and concentrated. The residue was purified by flash silica-gel column chromatography (PE/EA = 5/1, v/v) to afford product. Yields of **4a**-**4k** were determined after column chromatography.

*4.2.3.1. 2-((4-phenylthiazol-2-yl)thio)ethyl 2-bromoacetate (**4a**).* Colorless oil (1.93 g, yield 54 %). ^{1}H NMR (400 MHz, $CDCl_3$) δ 7.87 (d, J = 7.6 Hz, 2H), 7.42 (t, J = 7.5 Hz, 2H), 7.37–7.31 (m, 2H), 4.57 (t, J = 6.4 Hz, 2H), 3.82 (s, 2H), 3.59 (t, J = 6.4 Hz, 2H). ^{13}C NMR (100 MHz, $CDCl_3$) δ 167.1, 163.0, 155.5, 134.0, 128.9, 128.4, 126.4, 112.9, 64.6, 32.4, 25.7. HRMS (ESI), $C_{13}H_{12}BrNO_2S_2$ calcd for (M + H)$^+$ 357.9566, found 357.9568.

*4.2.3.2. 2-((4-(4-fluorophenyl)thiazol-2-yl)thio)ethyl 2-bromoacetate (**4b**).* Colorless oil (2.14 g, yield 57 %). ^{1}H NMR (400 MHz, $CDCl_3$) δ 7.84 (dd, J = 8.9, 5.4 Hz, 2H), 7.28 (s, 1H), 7.10 (t, J = 8.8 Hz, 2H), 4.56 (t, J = 6.4 Hz, 2H), 3.82 (s, 2H), 3.57 (t, J = 6.4 Hz, 2H). ^{13}C NMR (100 MHz, $CDCl_3$) δ 167.1, 164.1, 163.3, 161.7, 154.5, 130.3 (d, J = 3.3 Hz), 128.2 (d, J = 8.2 Hz), 115.9, 115.7, 112.4 (d, J = 1.3 Hz), 64.5, 32.4, 25.6. HRMS (ESI), $C_{13}H_{11}BrFNO_2S_2$ calcd for $(M + H)^+$ 375.9471, found 375.9480.

*4.2.3.3. 2-((4-(4-chlorophenyl)thiazol-2-yl)thio)ethyl 2-bromoacetate (**4c**).* Colorless oil (2.27 g, yield 58 %).^{1}H NMR (400 MHz, $CDCl_3$) δ 7.81–7.77 (m, 2H), 7.40–7.35 (m, 2H), 7.33 (s, 1H), 4.55 (t, J = 6.4 Hz, 2H), 3.82 (s, 2H), 3.57 (t, J = 6.4 Hz, 2H). ^{13}C NMR (100 MHz, $CDCl_3$) δ 167.0, 163.5, 154.2, 134.1, 132.4, 129.0, 127.6, 113.1, 64.4, 32.3, 25.6. HRMS (ESI), $C_{13}H_{11}BrClNO_2S_2$ calcd for $(M + H)^+$ 391.9176, found 391.9180.

*4.2.3.4. 2-((4-(3-chlorophenyl)thiazol-2-yl)thio)ethyl 2-bromoacetate (**4d**).* Colorless oil (2.20 g, yield 56 %). ^{1}H NMR (400 MHz, $CDCl_3$) δ 7.87 (t, J = 1.8 Hz, 1H), 7.74 (dt, J = 7.6, 1.5 Hz, 1H), 7.38 (s, 1H), 7.34 (d, J = 7.5 Hz, 1H), 7.30 (dt, J = 7.9, 1.6 Hz, 1H), 4.56 (t, J = 6.4 Hz, 2H), 3.83 (s, 2H), 3.60 (t, J = 6.4 Hz, 2H). ^{13}C NMR (100 MHz, $CDCl_3$) δ 167.1, 163.6, 154.0, 135.7, 134.9, 130.2, 128.4, 126.6, 124.5, 113.8, 64.5, 32.4, 25.6. HRMS (ESI), $C_{13}H_{11}BrClNO_2S_2$ calcd for $(M + H)^+$ 391.9176, found 391.9171.

*4.2.3.5. 2-((4-(4-bromophenyl)thiazol-2-yl)thio)ethyl 2-bromoacetate (**4e**).* White solid (2.58 g, yield 59 %).^{1}H NMR (400 MHz, $CDCl_3$) δ 7.74 (d, J = 8.7 Hz, 2H), 7.53 (d, J = 8.7 Hz, 2H), 7.35 (s, 1H), 4.56 (t, J = 6.4 Hz, 2H), 3.82 (s, 2H), 3.57 (t, J = 6.4 Hz, 2H). ^{13}C NMR (100 MHz, $CDCl_3$) δ 167.1, 163.6, 154.4, 132.9, 132.0, 127.9, 122.4, 113.3, 64.5, 32.4, 25.6. HRMS (ESI), $C_{13}H_{11}Br_2NO_2S_2$ calcd for $(M + H)^+$ 435.8671, found 435.8672.

*4.2.3.6. 2-((4-(3-bromophenyl)thiazol-2-yl)thio)ethyl 2-bromoacetate (**4f**).* White solid (2.57 g, yield 59 %). ^{1}H NMR (400 MHz, DMSO-d_6) δ 8.20 (s, 1H), 8.13 (t, J = 1.7 Hz, 1H), 7.96–7.93 (m, 1H), 7.54 (ddd, J = 7.9, 1.9, 0.9 Hz, 1H), 7.39 (d, J = 7.9 Hz, 1H), 4.47 (t, J = 6.2 Hz, 2H), 4.12 (s, 2H), 3.59 (t, J = 6.2 Hz, 2H). ^{13}C NMR (100 MHz, DMSO-d_6) δ 166.9, 163.6, 152.4, 135.7, 130.9, 130.8, 128.4, 124.9, 122.2, 116.0, 63.7, 32.2, 26.9. HRMS (ESI), $C_{13}H_{11}Br_2NO_2S_2$ calcd for $(M + H)^+$ 435.8671, found 435.8668.

*4.2.3.7. 2-((4-(p-tolyl)thiazol-2-yl)thio)ethyl 2-bromoacetate (**4g**).* Colorless oil (1.97 g, yield 53 %).^{1}H NMR (400 MHz, $CDCl_3$) δ 7.76 (d, J = 8.1 Hz, 2H), 7.29 (s, 1H), 7.22 (d, J = 8.1 Hz, 2H), 4.56 (t, J = 6.4 Hz, 2H), 3.82 (s, 2H), 3.57 (t, J = 6.4 Hz, 2H), 2.38 (s, 3H). ^{13}C NMR (100 MHz, $CDCl_3$) δ 167.0, 162.7, 155.5, 138.2, 131.3, 129.5, 126.2, 112.1, 64.5, 32.4, 25.7, 21.4. HRMS (ESI), $C_{14}H_{14}BrNO_2S_2$ calcd for $(M + H)^+$ 371.9722, found 371.9721.

*4.2.3.8. 2-((4-(4-methoxyphenyl)thiazol-2-yl)thio)ethyl 2-bromoacetate (**4h**).* Colorless oil (1.94 g, yield 50 %). ^{1}H NMR (400 MHz, $CDCl_3$) δ 7.80 (d, J = 8.9 Hz, 2H), 7.21 (s, 1H), 6.94 (d, J = 8.9 Hz, 2H), 4.56 (t, J = 6.4 Hz, 2H), 3.84 (s, 3H), 3.82 (s, 2H), 3.56 (t, J = 6.4 Hz, 2H). ^{13}C NMR (100 MHz, $CDCl_3$) δ 167.1, 162.8, 159.8, 155.3, 127.7, 126.9, 114.2, 111.1, 64.6, 55.5, 32.5, 25.6. HRMS (ESI), $C_{14}H_{14}BrNO_3S_2$ calcd for $(M + H)^+$ 387.9671, found 387.9670.

*4.2.3.9. 2-((4-(4-(trifluoromethyl)phenyl)thiazol-2-yl)thio)ethyl 2-bromoacetate (**4i**).* Colorless oil (2.22 g, yield 52 %).^{1}H NMR (400 MHz, $CDCl_3$) δ 7.98 (d, J = 8.1 Hz, 2H), 7.66 (d, J = 8.2 Hz, 2H), 7.46 (s, 1H), 4.57 (t, J = 6.5 Hz, 2H), 3.83 (s, 2H), 3.59 (t, J = 6.5 Hz, 2H). ^{13}C NMR (100 MHz, $CDCl_3$) δ 167.1, 163.9, 153.9, 137.1, 130.6, 130.3, 129.9, 129.7, 128.3, 126.6, 125.9 (q, J = 3.8 Hz), 125.6, 122.9, 114.6, 64.4, 32.3, 25.6. HRMS (ESI), $C_{14}H_{11}BrF_3NO_2S_2$ calcd for $(M + H)^+$ 425.9439, found 425.9434.

*4.2.3.10. 2-((4-(4-cyanophenyl)thiazol-2-yl)thio)ethyl 2-bromoacetate (**4j**).* White solid (2.29 g, yield 60 %). ^{1}H NMR (400 MHz, $CDCl_3$) δ 7.98 (d, J = 8.6 Hz, 2H), 7.70 (d, J = 8.6 Hz, 2H), 7.51 (s, 1H), 4.57 (t, J = 6.5 Hz, 2H), 3.83 (s, 2H), 3.60 (t, J = 6.5 Hz, 2H). ^{13}C NMR (100 MHz, $CDCl_3$) δ 167.1, 164.4, 153.4, 137.9, 132.8, 126.8, 118.9, 115.6, 111.7, 64.3, 32.3, 25.6. HRMS (ESI), $C_{14}H_{11}BrN_2O_2S_2$ calcd for $(M + H)^+$ 382.9518, found 382.9522.

*4.2.3.11. 2-((4-(4-nitrophenyl)thiazol-2-yl)thio)ethyl 2-bromoacetate (**4k**).* Yellow solid (1.73 g, yield 43 %). ^{1}H NMR (400 MHz, $CDCl_3$) δ 8.27 (d, J = 8.8 Hz, 2H), 8.03 (d, J = 8.4 Hz, 2H), 7.58 (s, 1H), 4.57 (t, J = 6.4 Hz, 2H), 3.83 (s, 2H), 3.61 (t, J = 6.5 Hz, 2H). ^{13}C NMR (100 MHz, $CDCl_3$) δ 167.1, 164.7, 152.9, 147.5, 139.7, 126.9, 124.3, 116.2, 64.3, 32.3, 25.6. HRMS (ESI), $C_{13}H_{11}BrN_2O_4S_2$ calcd for $(M + H)^+$ 402.9416, found 402.9415.

*4.2.4. General procedure for the synthesis of **5a**-**5k***

To a solution of ester **4a** (3 mmol) in CH_3CN (10 mL) was added triphenylphosphine (3.3 mmol). The mixture was stirred under room temperature overnight. The solvent was removed under reduced pressure and the residue was purified by flash silica-gel column chromatography (DCM/MeOH = 20/1, v/v) to afford product. Yields of **5a**-**5 k** were determined after column chromatography.

*4.2.4.1. (2-oxo-2-(2-((4-phenylthiazol-2-yl)thio)ethoxy)ethyl)triphenylphosphonium bromide (**5a**).* White solid (1.21 g, yield 65 %). ^{1}H NMR (400 MHz, DMSO-d_6) δ 8.06 (s, 1H), 7.82 (dd, J = 36.9, 23.7 Hz, 15H), 7.61 (dd, J = 21.3, 9.8 Hz, 2H), 7.42 (d, J = 7.7 Hz, 2H), 7.36 (t, J = 7.2 Hz, 1H), 5.40 (d, J = 14.5 Hz, 2H), 4.41 (t, J = 6.1 Hz, 2H), 3.36 (t, J = 6.2 Hz, 2H). ^{13}C NMR (100 MHz, DMSO-d_6) δ 164.5, 162.6, 154.1, 135.1 (d, J = 2.5 Hz), 133.7 (d, J = 10.8 Hz), 133.4, 130.1 (d, J = 13.0 Hz), 128.7, 128.2, 125.9, 118.0 (d, J = 88.0 Hz), 114.6, 63.8, 31.9, 29.4 (d, J = 56.6 Hz). ^{31}P NMR (162 MHz, $CDCl_3$) δ 20.6. HRMS (ESI), $C_{31}H_{27}NO_2PS_2$ calcd for M^+ 401.9337, found 401.9335.

*4.2.4.2. (2-(2-((4-(4-fluorophenyl)thiazol-2-yl)thio)ethoxy)-2-oxoethyl) triphenyl-phosphonium bromide (**5b**).* White solid (1.42 g, yield 74 %). ^{1}H NMR (400 MHz, $CDCl_3$) δ 7.93–7.85 (m, 6H), 7.78–7.73 (m, 5H), 7.68–7.61 (m, 6H), 7.36 (s, 1H), 7.32 (d, J = 8.6 Hz, 2H), 5.66 (d, J = 13.7 Hz, 2H), 4.40 (t, J = 6.3 Hz, 2H), 3.34 (t, J = 6.3 Hz, 2H). ^{13}C NMR (100 MHz, $CDCl_3$) δ 164.4, 163.1, 162.8, 160.7, 153.0, 135.0, 133.6 (d, J = 11.0 Hz), 130.0 (d, J = 13.0 Hz), 128.0 (d, J = 8.0 Hz), 118.1 (d, J = 89.0 Hz), 115.6 (d, J = 22.0 Hz), 114.3, 63.7, 54.8, 29.4 (d, J = 56.0 Hz). ^{31}P NMR (162 MHz, $CDCl_3$) δ 20.8. HRMS (ESI), $C_{31}H_{26}ClNO_2PS_2$ calcd for M^+ 574.0826, found 574.0836.

*4.2.4.3. (2-(2-((4-(4-chlorophenyl)thiazol-2-yl)thio)ethoxy)-2-oxoethyl) triphenyl-phosphonium bromide (**5c**).* White solid (1.45 g, yield 74 %). ^{1}H NMR (400 MHz, $CDCl_3$) δ 7.93–7.85 (m, 6H), 7.78–7.73 (m, 5H), 7.68–7.61 (m, 6H), 7.36 (s, 1H), 7.32 (d, J = 8.6 Hz, 2H), 5.66 (d, J = 13.7 Hz, 2H), 4.40 (t, J = 6.3 Hz, 2H), 3.34 (t, J = 6.3 Hz, 2H). ^{13}C NMR (100 MHz, $CDCl_3$) δ 164.6, 163.5, 154.1, 135.3 (d, J = 3.2 Hz), 134.2 (d, J = 10.8 Hz), 134.1, 132.3, 130.4 (d, J = 13.3 Hz), 129.0, 127.7, 118.0 (d, J = 88.0 Hz), 113.4, 64.7, 33.3 (d, J = 56.8 Hz), 32.4. ^{31}P NMR (162 MHz, $CDCl_3$) δ 20.81. HRMS (ESI), $C_{31}H_{26}ClNO_2PS_2$ calcd for M^+ 574.0826, found 574.0830.

*4.2.4.4. (2-(2-((4-(3-chlorophenyl)thiazol-2-yl)thio)ethoxy)-2-oxoethyl) triphenyl-phosphonium bromide (**5d**).* White solid (1.19 g, yield 61 %). ^{1}H NMR (400 MHz, $CDCl_3$) δ 7.92–7.85 (m, 6H), 7.80 (t, J = 1.9 Hz, 1H), 7.78–7.71 (m, 3H), 7.73–7.66 (m, 1H), 7.69–7.59 (m, 6H), 7.41 (s, 1H), 7.31 (t, J = 7.7 Hz, 1H), 7.28 (t, J = 1.8 Hz, 1H), 5.62 (d, J = 13.8 Hz,

2H), 4.39 (t, J = 6.3 Hz, 2H), 3.34 (t, J = 6.3 Hz, 2H). ^{13}C NMR (100 MHz, $CDCl_3$) δ 164.5, 163.6, 153.6, 135.5, 135.3 (d, J = 3.0 Hz), 134.8, 134.1 (d, J = 10.7 Hz), 130.4 (d, J = 13.2 Hz), 130.1, 128.3, 126.4, 124.5, 117.9 (d, J = 88.0 Hz), 114.2, 64.7, 33.3 (d, J = 56.7 Hz), 32.4. ^{31}P NMR (162 MHz, $CDCl_3$) δ 20.78. HRMS (ESI), $C_{31}H_{26}ClNO_2PS_2$ calcd for M^+ 574.0826, found 574.0821.

*4.2.4.5. (2-(2-((4-(4-bromophenyl)thiazol-2-yl)thio)ethoxy)-2-oxoethyl) triphenyl-phosphonium bromide (**5e**).* White solid (0.98 g, 47 % yield). ^{1}H NMR (400 MHz, DMSO-d_6) δ 8.13 (s, 1H), 7.92–7.85 (m, 6H), 7.84–7.79 (m, 5H), 7.78–7.72 (m, 6H), 7.61 (d, J = 8.6 Hz, 2H), 5.41 (d, J = 14.5 Hz, 2H), 4.40 (t, J = 6.1 Hz, 2H), 3.36 (t, J = 6.2 Hz, 2H). ^{13}C NMR (100 MHz, DMSO-d_6) δ 164.4, 163.0, 152.8, 135.0 (d, J = 2.9 Hz), 133.6 (d, J = 10.8 Hz), 132.6, 131.6, 130.0 (d, J = 13.0 Hz), 127.9, 121.3, 118.3 (d, J = 88.9 Hz), 115.3, 63.7, 31.9, 29.3 (d, J = 56.4 Hz). ^{31}P NMR (162 MHz, $CDCl_3$) δ 20.5. HRMS (ESI), $C_{31}H_{26}BrNO_2PS_2$ calcd for M^+ 618.0320, found 618.0329.

*4.2.4.6. (2-(2-((4-(3-bromophenyl)thiazol-2-yl)thio)ethoxy)-2-oxoethyl) triphenyl-phosphonium bromide (**5f**).* White solid (1.02 g, 49 % yield). ^{1}H NMR (400 MHz, $CDCl_3$) δ 7.97 (t, J = 1.8 Hz, 1H), 7.94–7.84 (m, 6H), 7.78–7.74 (m, 4H), 7.65 (td, J = 7.7, 3.6 Hz, 6H), 7.48–7.41 (m, 2H), 7.26 (t, J = 7.9 Hz, 1H). 5.64 (d, J = 13.7 Hz, 2H), 4.40 (t, J = 6.2 Hz, 2H), 3.36 (t, J = 6.2 Hz, 2H). ^{13}C NMR (100 MHz, $CDCl_3$) δ 164.5, 164.0, 153.3, 135.5, 135.3 (d, J = 3.2 Hz), 134.1 (d, J = 10.8 Hz), 131.4, 130.5, 130.3, 129.3, 124.9, 123.0, 117.9 (d, J = 89.0 Hz), 114.5, 64.8, 33.3 (d, J = 56.5 Hz), 32.5. ^{31}P NMR (162 MHz, $CDCl_3$) δ 20.48. HRMS (ESI), $C_{31}H_{26}BrNO_2PS_2$ calcd for M^+ 618.0320, found 618.0314.

*4.2.4.7. (2-oxo-2-(2-((4-(p-tolyl)thiazol-2-yl)thio)ethoxy)ethyl)triphenyl-phosphonium bromide (**5 g**).* White solid (0.97 g, yield 51 %). ^{1}H NMR (400 MHz, $CDCl_3$) δ 7.75 (dd, J = 12.1, 7.8 Hz, 6H), 7.67–7.60 (m, 5H), 7.55 (s, 6H), 7.23 (s, 1H), 7.08 (d, J = 8.0 Hz, 2H), 5.38 (s, 2H), 4.28 (t, J = 5.9 Hz, 2H), 3.21 (t, J = 6.1 Hz, 2H), 2.27 (s, 3H). ^{13}C NMR (100 MHz, $CDCl_3$) δ 164.0, 162.3, 155.1, 137.9, 135.0, 133.7 (d, J = 10.3 Hz), 130.9, 130.1 (d, J = 10.1 Hz), 129.2, 125.9, 117.5 (d, J = 98.6 Hz), 112.1, 64.4, 32.8 (d, J = 54.2 Hz), 32.1, 21.1. ^{31}P NMR (162 MHz, $CDCl_3$) δ 20.6. HRMS (ESI), $C_{32}H_{29}NO_2PS_2$ calcd for M^+ 554.1372, found 554.1370.

*4.2.4.8. (2-(2-((4-(4-methoxyphenyl)thiazol-2-yl)thio)ethoxy)-2-oxoethyl)triphenyl-phosphonium bromide (**5h**).* White solid (1.28 g, yield 66 %). ^{1}H NMR (400 MHz, $CDCl_3$) δ 7.91–7.81 (m, 6H), 7.77–7.70 (m, 5H), 7.65–7.60 (m, 6H), 7.20 (s, 1H), 5.57 (s, 2H), 6.89 (d, J = 8.8 Hz, 2H), 4.38 (t, J = 6.2 Hz, 2H), 3.82 (s, 3H), 3.30 (t, J = 6.2 Hz, 2H). ^{13}C NMR (100 MHz, $CDCl_3$) δ 164.5, 162.5, 159.8, 155.2, 135.2 (d, J = 3.0 Hz), 134.1 (d, J = 10.8 Hz), 130.3 (d, J = 13.2 Hz), 127.6, 126.8, 118.0 (d, J = 88.9 Hz), 114.2, 111.2, 64.7, 55.4, 33.1 (d, J = 56.8 Hz), 32.4. ^{31}P NMR (162 MHz, $CDCl_3$) δ 20.74. HRMS (ESI), $C_{32}H_{29}NO_3PS_2$ calcd for M^+ 570.1321, found 570.1328.

*4.2.4.9. (2-oxo-2-(2-((4-(4-(trifluoromethyl)phenyl)thiazol-2-yl)thio) ethoxy)ethyl)-triphenylphosphonium bromide (**5i**).* White solid (1.56 g, yield 76 %). ^{1}H NMR (400 MHz, $CDCl_3$) δ 7.89 (d, J = 8.2 Hz, 2H), 7.81 (dd, J = 13.5, 7.3 Hz, 6H), 7.73–7.68 (m, 3H), 7.62–7.56 (m, 6H), 7.54–7.50 (m, 3H), 5.49 (s, 2H), 4.34 (t, J = 6.3 Hz, 2H), 3.28 (t, J = 6.4 Hz, 2H). ^{13}C NMR (100 MHz, $CDCl_3$) δ 163.6, 162.8, 152.7, 136.5, 134.8 (d, J = 3.1 Hz), 133.3 (d, J = 10.8 Hz), 129.8 (d, J = 13.2 Hz), 128.9 (q, J = 32.3 Hz), 127.7, 125.0 (d, J = 3.8 Hz), 124.9, 122.2, 121.0, 117.50, 116.6, 115.3, 63.9, 32.3 (d, J = 56.4 Hz), 31.6. ^{31}P NMR (162 MHz, $CDCl_3$) δ 20.5. HRMS (ESI), $C_{32}H_{26}F_3NO_2PS_2$ calcd for M + 608.1089, found 608.1089.

*4.2.4.10. (2-(2-((4-(4-cyanophenyl)thiazol-2-yl)thio)ethoxy)-2-oxoethyl) triphenyl-phosphonium bromide (**5j**).* White solid (1.18 g, yield 61 %). ^{1}H NMR (400 MHz, $CDCl_3$) δ 7.89 (d, J = 8.4 Hz, 2H), 7.80–7.71 (m, 6H), 7.68–7.61 (m, 4H), 7.54 (d, J = 9.2 Hz, 7H), 7.51 (s, 1H), 5.40 (s, 2H), 4.29 (t, J = 6.1 Hz, 2H), 3.25 (t, J = 6.3 Hz, 2H). ^{13}C NMR (100 MHz, $CDCl_3$) δ 163.7, 152.7, 137.6, 135.0, 133.7 (d, J = 9.9 Hz), 132.3, 131.7, 130.0, 128.4, 126.6, 118.7, 116.3, 110.9, 64.0, 32.9, 32.0. ^{31}P NMR (162 MHz, $CDCl_3$) δ 20.5. HRMS (ESI), $C_{32}H_{26}N_2O_2PS_2$ calcd for M^+ 565.1168, found 565.1171.

*4.2.4.11. (2-(2-((4-(4-nitrophenyl)thiazol-2-yl)thio)ethoxy)-2-oxoethyl) triphenyl-phosphonium bromide (**5k**).* White solid (1.55 g, yield 78 %). ^{1}H NMR (400 MHz, $CDCl_3$) δ 8.18 (d, J = 2.0 Hz, 2H), 8.00 (d, J = 3.0 Hz, 2H), 7.93–7.85 (m, 6H), 7.79–7.73 (m, 3H), 7.69–7.62 (m, 7H), 5.68 (d, J = 3.0 Hz, 2H), 4.42 (d, J = 2.0 Hz, 2H), 3.38 (d, J = 2.0 Hz, 2H). ^{13}C NMR (100 MHz, $CDCl_3$) δ 164.6, 152.7, 147.2, 139.7, 135.3, 134.1 (d, J = 10.3 Hz), 132.2, 130.4 (d, J = 13.5 Hz), 126.9, 124.2, 117.9 (d, J = 89.0 Hz), 116.8, 64.5, 33.5, 32.1. ^{31}P NMR (162 MHz, $CDCl_3$) δ 20.7. HRMS (ESI), $C_{31}H_{26}N_2O_4PS_2$ calcd for M^+ 585.1066, found 585.1072.

*4.2.5. General procedure for the synthesis of **6a** and **6b***

To a solution of **3 l** (5 mmol) in CH_3CN (30 mL) was added benzyl bromide (for **6a**) or 1-(bromomethyl)-4-chlorobenzene (for **6b**) (3.3 mmol) and potassium carbonate (6 mmol). The mixture was stirred under 80 ℃ for 16 h. The solvent was removed under vaccum and the residue was purified by flash silica-gel column chromatography (PE/EA = 2/1, v/v) to afford product. Yields of **6a** and **6b** were determined after column chromatography.

*4.2.5.1. 2-((4-(4-(benzyloxy)phenyl)thiazol-2-yl)thio)ethan-1-ol (**6a**).* White solid (1.35 g, yield 79 %). ^{1}H NMR (400 MHz, DMSO-d_6) δ 7.88–7.83 (m, 3H), 7.47 (d, J = 6.9 Hz, 2H), 7.40 (t, J = 7.3 Hz, 2H), 7.34 (t, J = 7.2 Hz, 1H), 7.08 (d, J = 8.9 Hz, 2H), 5.15 (s, 2H), 5.11 (t, J = 5.5 Hz, 1H), 3.74 (dd, J = 12.0, 6.4 Hz, 2H), 3.36 (d, J = 6.4 Hz, 2H). ^{13}C NMR (100 MHz, DMSO-d_6) δ 164.1, 158.3, 153.9, 136.9, 128.4, 127.8, 127.6, 127.3, 126.7, 114.9, 111.9, 69.3, 59.6, 36.6. HRMS (ESI), $C_{18}H_{17}NO_2S_2$ calcd for $(M + H)^+$ 344.0773, found 344.0773.

*4.2.5.2. 2-((4-(4-((4-chlorobenzyl)oxy)phenyl)thiazol-2-yl)thio)ethan-1-ol (**6b**).* White solid (1.47 g, yield 78 %). ^{1}H NMR (400 MHz, $CDCl_3$) δ 7.74 (d, J = 8.9 Hz, 2H), 7.36 (s, 4H), 7.21 (s, 1H), 6.98 (d, J = 8.9 Hz, 2H), 5.05 (s, 2H), 4.07–4.04 (m, 2H), 3.41–3.38 (m, 2H). ^{13}C NMR (100 MHz, $CDCl_3$) δ 164.8, 158.8, 155.0, 135.4, 133.9, 128.92, 128.90, 127.7, 127.0, 115.3, 111.8, 69.4, 63.1, 37.7. HRMS (ESI), $C_{18}H_{16}ClNO_2S_2$ calcd for $(M + H)^+$ 378.0384, found 378.0379.

*4.2.6. General procedure for the synthesis of **7a** and **7b***

To a stirred solution of compound **6a** or **6b** (3 mmol) in 20 mL DCM under ice bath was added bromoacetyl bromide (3.6 mmol). The reaction mixture was stirred for 2 h under room temperature and washed by saturated aqueous $NaHCO_3$ and brine, dried over by anhydrous Na_2SO_4 and concentrated. The residue was purified by flash silica-gel column chromatography (PE/EA = 5/1, v/v) to afford product. Yields of **7a** and **7b** were determined after column chromatography.

*4.2.6.1. 2-((4-(4-(benzyloxy)phenyl)thiazol-2-yl)thio)ethyl 2-bromoacetate (**7a**).* White solid (1.39 g, yield 63 %). ^{1}H NMR (400 MHz, DMSO-d_6) δ 7.89–7.85 (m, 3H), 7.47 (d, J = 7.3 Hz, 2H), 7.40 (t, J = 7.4 Hz, 2H), 7.34 (d, J = 7.1 Hz, 1H), 7.08 (d, J = 8.8 Hz, 2H), 5.15 (s, 2H), 4.48 (t, J = 6.3 Hz, 2H), 4.13 (s, 2H), 3.57 (t, J = 6.3 Hz, 2H). ^{13}C NMR (100 MHz, DMSO-d_6) δ 166.9, 162.7, 158.3, 154.1, 136.9, 128.4, 127.8, 127.7, 127.3, 126.6, 115.0, 112.5, 69.3, 63.7, 32.1, 26.8. HRMS (ESI), $C_{20}H_{18}BrNO_3S_2$ calcd for $(M + H)^+$ 463.9984, found 463.9981.

*4.2.6.2. 2-((4-(4-((4-chlorobenzyl)oxy)phenyl)thiazol-2-yl)thio)ethyl 2-bromoacetate (**7b**).* White solid (1.12 g, yield 75 %). ^{1}H NMR (400 MHz, $CDCl_3$) δ 7.81 (d, J = 8.5 Hz, 2H), 7.45–7.30 (m, 4H), 7.23 (s, 1H),

6.99 (d, J = 8.6 Hz, 2H), 5.07 (s, 2H), 4.56 (t, J = 6.4 Hz, 2H), 3.82 (s, 2H), 3.57 (t, J = 6.4 Hz, 2H). ^{13}C NMR (100 MHz, $CDCl_3$) δ 167.1, 162.8, 158.8, 155.2, 135.5, 133.9, 128.92, 128.91, 127.8, 127.5, 115.2, 111.3, 69.4, 64.6, 32.4, 25.7. HRMS (ESI), $C_{20}H_{17}ClBrNO_3S_2$ calcd for $(M + H)^+$ 497.9595, found 497.9596.

*4.2.7. General procedure for the synthesis of **8a** and **8b***

To a solution of ester **7a** or **7b** (3 mmol) in CH_3CN (10 mL) was added triphenylphosphine (3.3 mmol). The mixture was stirred under room temperature overnight. The solvent was removed under reduced pressure and the residue was purified by flash silica-gel column chromatography (DCM/MeOH = 20/1, v/v) to afford product. Yields of **8a** and **8b** were determined after column chromatography.

*4.2.7.1. (2-(2-((4-(4-(benzyloxy)phenyl)thiazol-2-yl)thio)ethoxy)-2-oxoethyl)-triphenylphosphonium bromide (**8a**).* White solid (1.52 g, yield 70 %). ^{1}H NMR (400 MHz, DMSO-d_6) δ 7.91–7.80 (m, 10*H*), 7.77–7.75 (m, 5H), 7.68–7.52 (m, 3H), 7.47 (d, J = 7.3 Hz, 2H), 7.40 (t, J = 7.4 Hz, 2H), 7.33 (t, J = 7.2 Hz, 1H), 7.06 (d, J = 8.7 Hz, 2H), 5.44 (d, J = 14.5 Hz, 2H), 5.15 (s, 2H), 4.40 (t, J = 5.9 Hz, 2H), 3.34 (t, J = 5.9 Hz, 2H). ^{13}C NMR (100 MHz, DMSO-d_6) δ 164.4 (d, J = 3.2 Hz), 162.2, 158.3, 153.9, 136.8, 135.0, 133.6 (d, J = 10.8 Hz), 130.0 (d, J = 13.1 Hz), 128.3, 127.8, 127.6, 127.3, 126.5, 118.0 (d, J = 88.8 Hz), 114.9, 112.5, 69.2, 63.8, 54.8, 30.8 (d, J = 217.0 Hz). ^{31}P NMR (162 MHz, $CDCl_3$) δ 20.7. HRMS (ESI), $C_{38}H_{33}NO_3PS_2$ calcd for M^+ 646.1634, found 646.1634.

*4.2.7.2. (2-(2-((4-(4-((4-chlorobenzyl)oxy)phenyl)thiazol-2-yl)thio)ethoxy)-2-oxoethyl)triphenylphosphonium bromide (**8b**).* White solid (1.46 g, yield 64 %). ^{1}H NMR (400 MHz, $CDCl_3$) δ 7.91–7.83 (m, 6H), 7.77–7.71 (m, 5H), 7.66–7.60 (m, 6H) 7.38–7.32 (m, 4H), 7.21 (s, 1H), 6.95 (d, J = 8.8 Hz, 2H), 5.62 (d, J = 16.0 Hz, 2H), 5.05 (s, 2H), 4.38 (t, J = 6.0 Hz, 2H), 3.31 (t, J = 6.0 Hz, 2H). ^{13}C NMR (100 MHz, CDCl3) δ 164.5, 162.6, 158.7, 155.0, 135.4, 135.2 (d, J = 3.0 Hz), 134.1 (d, J = 10.7 Hz), 133.9, 133.0, 130.3 (d, J = 13.3 Hz), 128.8 (d, J = 1.7 Hz), 127.7, 127.3, 117.9 (d, J = 88.0 Hz), 115.1, 111.3, 69.3, 64.7, 33.2 (d, J = 56.5 Hz), 32.3. ^{31}P NMR (162 MHz, $CDCl_3$) δ 20.8. HRMS (ESI), $C_{38}H_{32}ClNO_3PS_2$ calcd for M^+ 680.1244, found 680.1233.

*4.2.8. General procedure for the synthesis of **9a**-**9f***

To a solution of 1-ethyl-3(3-dimethylpropylamine) carbodiimide (EDCI) (6 mmol) with (3-carboxypropyl)triphenylphosphonium bromide (6 mmol) in DCM (20 mL) was added compound **3a** (2 mmol) and DMAP (2 mmol) under ice bath. The solution was warmed to room temperature and stirred for 3 h. The solvent was removed under reduced pressure and the product was purified by flash silica-gel column chromatography (DCM/MeOH = 20/1, v/v) to afford product. Yields of **9a**-**9k** were determined after column chromatography.

*4.2.8.1. (4-oxo-4-(2-((4-phenylthiazol-2-yl)thio)ethoxy)butyl)triphenyl-phosphonium bromide (**9a**).* White solid (0.71 g, yield 55 %). ^{1}H NMR (400 MHz, $CDCl_3$) δ 7.89–7.82 (m, 8H), 7.79–7.73 (m, 3H), 7.70–7.62 (m, 6H), 7.38–7.33 (m, 3H), 7.29 (d, J = 7.3 Hz, 1H), 4.43 (t, J = 6.5 Hz, 2H), 4.09–3.98 (m, 2H), 3.50 (t, J = 6.5 Hz, 2H), 2.92–2.88 (m, 2H), 1.93–1.88 (m, 2H). ^{13}C NMR (100 MHz, $CDCl_3$) δ 173.0, 163.3, 155.3, 134.0, 135.0 (d, J = 2.9 Hz), 133.9 (d, J = 10.1 Hz), 130.5 (d, J = 12.5 Hz), 128.8, 128.2, 126.3, 118.3 (d, J = 85.0 Hz), 112.9, 63.0, 33.1, 32.7, 21.7 (d, J = 51.3 Hz), 18.1. ^{31}P NMR (162 MHz, $CDCl_3$) δ 24.3. HRMS (ESI), $C_{40}H_{37}NO_3PS_2$ calcd for M^+ 674.1947, found 674.1950.

*4.2.8.2. (4-(2-((4-(4-fluorophenyl)thiazol-2-yl)thio)ethoxy)-4-oxobutyl) triphenyl-phosphonium bromide (**9b**).* White solid (0.67 g, yield 50 %).^{1}H NMR (400 MHz, $CDCl_3$) δ 7.81–7.75 (m, 8H), 7.75–7.69 (m, 3H), 7.66–7.60 (m, 6H), 7.29 (s, 1H), 6.97 (t, J = 8.7 Hz, 2H), 4.37 (t, J = 6.4 Hz, 2H), 3.96–3.87 (m, 2H), 3.43 (t, J = 6.5 Hz, 2H), 2.82 (t, J = 6.5 Hz, 2H), 1.89–1.75 (m, 2H). ^{13}C NMR (100 MHz, $CDCl_3$) δ 172.7, 163.8, 163.4, 161.3, 154.1, 135.0 (d, J = 3.0 Hz), 133.6 (d, J = 10.0 Hz), 130.4 (d, J = 12.5 Hz), 128.0 (d, J = 8.2 Hz), 118.0 (d, J = 85.0 Hz), 115.5, 112.6, 62.9, 33.1 (d, J = 18.3 Hz), 32.5, 21.5 (d, J = 51.5 Hz), 17.9 (d, J = 3.1 Hz). ^{31}P NMR (162 MHz, $CDCl_3$) δ 24.1. HRMS (ESI), $C_{40}H_{36}FNO_3PS_2$ calcd for M^+ 692.1853, found 692.1856.

*4.2.8.3. (4-(2-((4-(4-chlorophenyl)thiazol-2-yl)thio)ethoxy)-4-oxobutyl)-triphenylphosphonium bromide (**9c**).* White solid (0.75 g, yield 55 %). ^{1}H NMR (400 MHz, $CDCl_3$) δ 7.80–7.76 (m, 4H), 7.75–7.69 (m, 7H), 7.65–7.59 (m, 6H), 7.36 (s, 1H), 7.23 (d, J = 8.6 Hz, 2H), 4.36 (t, J = 6.5 Hz, 2H), 3.94–3.82 (m, 2H), 3.43 (t, J = 6.4 Hz, 2H), 2.80 (t, J = 6.5 Hz, 2H), 1.86–1.76 (m, 2H). ^{13}C NMR (100 MHz, $CDCl_3$) δ 172.6, 163.5, 153.8, 135.0 (d, J = 3.0 Hz), 133.7, 133.6 (d, J = 10.0 Hz), 132.3, 130.4 (d, J = 12.6 Hz), 128.7, 127.5, 117.9 (d, J = 85.0 Hz), 113.4, 62.8, 33.1 (d, J = 18.3 Hz), 32.5, 21.6 (d, J = 51.6 Hz), 17.9 (d, J = 3.2 Hz). ^{31}P NMR (162 MHz, $CDCl_3$) δ 24.1. HRMS (ESI), $C_{40}H_{36}ClNO_3PS_2$ calcd for M^+ 708.1557, found 708.1554.

*4.2.8.4. (4-oxo-4-(2-((4-(p-tolyl)thiazol-2-yl)thio)ethoxy)butyl)triphenyl-phosphonium bromide (**9d**).* White solid (0.41 g, yield 31 %). ^{1}H NMR (400 MHz, $CDCl_3$) δ 7.89–7.82 (m, 7H), 7.77–7.72 (m, 4H), 7.70–7.65 (m, 6H), 7.29 (s, 1H), 7.16 (d, J = 7.9 Hz, 2H), 4.42 (t, J = 6.4 Hz, 2H), 4.09–3.99 (m, 2H), 3.50 (t, J = 6.5 Hz, 2H), 2.89 (t, J = 6.5 Hz, 2H), 2.34 (s, 3H), 1.96–1.83 (m, 2H). ^{13}C NMR (100 MHz, $CDCl_3$) δ 172.9, 163.1, 155.4, 138.1, 135.0 (d, J = 3.0 Hz), 133.8 (d, J = 10.2 Hz), 131.3, 130.5 (d, J = 12.5 Hz), 129.4, 126.2, 118.2 (d, J = 86.0 Hz), 112.2, 63.0, 33.2 (d, J = 18.5 Hz), 32.7, 21.7 (d, J = 51.2 Hz), 21.3, 18.1. ^{31}P NMR (162 MHz, $CDCl_3$) δ 24.2. HRMS (ESI), $C_{41}H_{39}NO_3PS_2$ calcd for M^+ 688.2103, found 688.2101.

*4.2.8.5. (4-(2-((4-(4-methoxyphenyl)thiazol-2-yl)thio)ethoxy)-4-oxobutyl)triphenyl-phosphonium bromide (**9e**).* White solid (0.40 g, yield 30 %). ^{1}H NMR (400 MHz, $CDCl_3$) δ 7.85–7.75 (m, 6H), 7.78–7.69 (m, 5H), 7.68–7.59 (m, 6H), 7.19 (s, 1H), 6.85 (d, J = 7.3 Hz, 2H), 4.38 (t, J = 6.4 Hz, 2H), 4.00–3.91 (m, 2H), 3.77 (s, 3H), 3.44 (t, J = 6.5 Hz, 2H), 2.84 (t, J = 6.6 Hz, 2H), 1.89–1.81 (m, 2H). ^{13}C NMR (100 MHz, $CDCl_3$) δ 171.5, 161.8, 158.6, 153.9, 134.2 (d, J = 3.6 Hz), 132.6 (d, J = 10.0 Hz), 129.6 (d, J = 12.7 Hz), 126.7, 125.8, 116.9 (d, J = 86.0 Hz), 113.1, 110.6, 61.9, 54.5, 32.3 (d, J = 18.4 Hz), 31.7, 20.5 (d, J = 51.7 Hz), 17.0. ^{31}P NMR (162 MHz, $CDCl_3$) δ 23.5. HRMS (ESI), HRMS (ESI), $C_{41}H_{39}NO_4PS_2$ calcd for M^+ 704.2053, found 704.2053.

*4.2.8.6. (4-oxo-4-(2-((4-(4-(trifluoromethyl)phenyl)thiazol-2-yl)thio) ethoxy)butyl)-triphenylphosphonium bromide (**9f**).* White solid (1.03 g, yield 72 %). ^{1}H NMR (400 MHz, $CDCl_3$) δ 7.96 (d, J = 8.1 Hz, 2H), 7.87–7.79 (m, 6H), 7.78–7.71 (m, 3H), 7.69–7.62 (m, 6H), 7.58 (d, J = 8.2 Hz, 2H), 7.52 (s, 1H), 4.42 (t, J = 6.4 Hz, 2H), 4.11–3.90 (m, 2H), 3.49 (t, J = 6.5 Hz, 2H), 2.87 (t, J = 6.5 Hz, 2H), 1.92–1.82 (m, 2H). ^{13}C NMR (100 MHz, $CDCl_3$) δ 172.9, 164.2, 153.6, 137.1, 135.0 (d, J = 3.0 Hz), 133.8 (d, J = 10.0 Hz), 130.5 (d, J = 12.6 Hz), 130.3, 130.0, 129.7, 129.3, 128.2, 126.5, 125.7 (q, J = 3.8 Hz), 125.5, 122.8, 120.1, 118.3 (d, J = 85.0 Hz), 115.0, 62.9, 33.2 (d, J = 18.5 Hz), 32.6, 21.5 (d, J = 51.4 Hz), 18.0 (d, J = 3.2 Hz). ^{31}P NMR (162 MHz, $CDCl_3$) δ 23.5. HRMS (ESI), $C_{41}H_{36}F_3NO_3PS_2$ calcd for M^+ 742.1821, found 742.1820.

*4.2.9. General procedure for the synthesis of **10a**-**10c***

Thiazole-2-thiol (**3a**) (5 mmol), 4-bromo-1-butanol (6 mmol) and potassium carbonate (6 mmol) were dissolved in acetone (20 mL) and stirred for 4 h. The solvent was removed under reduced pressure. The residue was purified by flash silica-gel column chromatography (PE/EA = 3/1, v/v). Yields of **10a**-**10c** were determined after column chromatography.

*4.2.9.1. 4-((4-(4-chlorophenyl)thiazol-2-yl)thio)butan-1-ol (**10a**).* White

solid (1.18 g, yield 79 %). ^{1}H NMR (400 MHz, $CDCl_3$) δ 7.79 (d, J = 8.4 Hz, 2H), 7.37 (d, J = 8.4 Hz, 2H), 7.31 (s, 1H), 3.69 (t, J = 6.3 Hz, 2H), 3.30 (t, J = 7.2 Hz, 2H), 1.94–1.88 (m, 2H), 1.74 (dd, J = 13.4, 5.1 Hz, 3H). ^{13}C NMR (100 MHz, $CDCl_3$) δ 165.5, 154.3, 134.1, 132.7, 128.9, 127.7, 112.7, 62.3, 34.4, 31.7, 25.9. HRMS (ESI), $C_{13}H_{14}ClNOS_2$ calcd for $(M + H)^+$ 300.0278, found 300.0283.

*4.2.9.2. 6-((4-(4-chlorophenyl)thiazol-2-yl)thio)hexan-1-ol (**10b**).* White solid (1.32 g, yield 81 %). ^{1}H NMR (400 MHz, $CDCl_3$) δ 7.79 (d, J = 8.4 Hz, 2H), 7.36 (d, J = 8.4 Hz, 2H), 7.31 (s, 1H), 3.62 (t, J = 6.5 Hz, 2H), 3.24 (t, J = 7.3 Hz, 2H), 1.83–1.78 (m, 2H), 1.70 (s, 1H), 1.58–1.54 (m, 2H), 1.48 (d, J = 7.7 Hz, 2H), 1.41 (d, J = 6.8 Hz, 2H). ^{13}C NMR (100 MHz, $CDCl_3$) δ 165.6, 154.2, 133.9, 132.7, 128.9, 127.6, 112.6, 62.8, 34.5, 32.6, 29.3, 28.6, 25.4. HRMS (ESI), $C_{15}H_{18}ClNOS_2$ calcd for $(M + H)^+$ 328.0591, found 328.0591.

*4.2.9.3. 8-((4-(4-chlorophenyl)thiazol-2-yl)thio)octan-1-ol (**10c**).* White solid (1.37 g, yield 77 %). ^{1}H NMR (400 MHz, $CDCl_3$) δ 7.81 (d, J = 8.7 Hz, 2H), 7.37 (d, J = 8.7 Hz, 2H), 7.32 (s, 1H), 3.62 (t, J = 6.6 Hz, 2H), 3.27–3.23 (m, 2H), 1.83–1.77 (m, 2H), 1.57–1.52 (m, 2H), 1.49–1.43 (m, 2H), 1.36–1.32 (m, 6H). ^{13}C NMR (100 MHz, $CDCl_3$) δ 165.7, 154.3, 134.0, 132.8, 128.9, 127.7, 112.6, 63.1, 34.7, 32.9, 29.4, 29.3, 29.1, 28.8, 25.8. HRMS (ESI), $C_{17}H_{22}ClNOS_2$ calcd for $(M + H)^+$ 356.0904, found 356.0901.

*4.2.10. General procedure for the synthesis of **11a-11c***

To a stirred solution of compound **10a** (5 mmol) in 20 mL DCM under ice bath was added bromoacetyl bromide (6 mmol). The reaction mixture was stirred for 2 h under room temperature and washed by saturated aqueous $NaHCO_3$ and brine, dried over by anhydrous Na_2SO_4 and concentrated. The residue was purified by flash silica-gel column chromatography (PE/EA = 5/1, v/v) to afford product. Yields of **11a-11c** were determined after column chromatography.

*4.2.10.1. 4-((4-(4-chlorophenyl)thiazol-2-yl)thio)butyl 2-bromoacetate (**11a**).* White solid (1.55 g, yield 74 %). ^{1}H NMR (400 MHz, $CDCl_3$) δ 7.81 (d, J = 8.3 Hz, 2H), 7.38 (d, J = 8.3 Hz, 2H), 7.33 (s, 1H), 4.23 (t, J = 6.0 Hz, 2H), 3.81 (s, 2H), 3.32 (t, J = 6.7 Hz, 2H), 1.94–1.85 (m, 4H). ^{13}C NMR (100 MHz, $CDCl_3$) δ 167.4, 164.9, 154.3, 134.1, 132.7, 129.0, 127.7, 112.8, 65.7, 34.0, 27.6, 25.9, 25.8. HRMS (ESI), $C_{15}H_{15}BrClNO_2S_2$ calcd for $(M + H)^+$ 419.9489, found 419.9492.

*4.2.10.2. 6-((4-(4-chlorophenyl)thiazol-2-yl)thio)hexyl 2-bromoacetate (**11b**).* White solid (1.66 g, yield 74 %). ^{1}H NMR (400 MHz, $CDCl_3$) δ 7.81 (d, J = 8.7 Hz, 2H), 7.37 (d, J = 8.7 Hz, 2H), 7.33 (s, 1H), 4.17 (t, J = 6.6 Hz, 2H), 3.82 (s, 2H), 3.29–3.25 (m, 2H), 1.85–1.80 (m, 2H), 1.71–1.66 (m, 2H), 1.54–1.48 (m, 2H), 1.43 (dd, J = 13.1, 6.2 Hz, 2H). ^{13}C NMR (100 MHz, $CDCl_3$) δ 167.4, 165.4, 154.3, 134.0, 132.8, 128.9, 127.7, 112.6, 66.3, 34.5, 29.2, 28.4, 28.3, 25.9, 25.4. HRMS (ESI), $C_{17}H_{19}BrClNO_2S_2$ calcd for $(M + H)^+$ 447.9802, found 447.9812.

*4.2.10.3. 8-((4-(4-chlorophenyl)thiazol-2-yl)thio)octyl 2-bromoacetate (**11c**).* White solid (1.69 g, yield 71 %). ^{1}H NMR (400 MHz, $CDCl_3$) δ 7.81 (d, J = 8.6 Hz, 2H), 7.37 (d, J = 8.6 Hz, 2H), 7.32 (s, 1H), 4.15 (t, J = 6.7 Hz, 2H), 3.82 (s, 2H), 3.25 (t, J = 7.3 Hz, 2H), 1.83–1.77 (m, 2H), 1.67–1.63 (m, 2H), 1.49–1.43 (m, 2H), 1.34 (d, J = 1.4 Hz, 6H). ^{13}C NMR (100 MHz, $CDCl_3$) δ 167.4, 165.6, 164.7, 154.2, 133.9, 132.8, 128.9, 127.7, 112.6, 66.5, 29.3, 29.1, 29.0, 28.7, 28.5, 26.1, 25.8. HRMS (ESI), $C_{19}H_{23}BrClNO_2S_2$ calcd for $(M + H)^+$ 476.0115, found 476.0110.

*4.2.11. General procedure for the synthesis of **12a-12c***

To a solution of ester **11a** (3 mmol) in CH_3CN (10 mL) was added triphenylphosphine (3.3 mmol). The mixture was stirred under room temperature overnight. The solvent was removed under reduced pressure and the residue was purified by flash silica-gel column chromatography (DCM/MeOH = 20/1, v/v) to afford product. Yields of **12a-12c** were determined after column chromatography.

*4.2.11.1. (2-(4-((4-(4-chlorophenyl)thiazol-2-yl)thio)butoxy)-2-oxoethyl)-triphenylphosphonium bromide (**12a**).* White solid (1.86 g, yield 91 %). ^{1}H NMR (400 MHz, $CDCl_3$) δ 7.76 (ddd, J = 22.0, 13.3, 7.4 Hz, 11*H*), 7.64–7.58 (m, 6H), 7.36 (s, 1H), 7.28 (d, J = 8.6 Hz, 2H), 5.45 (d, J = 12.6 Hz, 2H), 3.97 (t, J = 5.9 Hz, 2H), 3.13 (t, J = 6.6 Hz, 2H), 1.61 (d, J = 5.0 Hz, 4H). ^{13}C NMR (100 MHz, $CDCl_3$) δ 164.9, 154.1, 135.3, 134.0 (d, J = 11.1 Hz), 133.9, 132.6, 130.3 (d, J = 13.1 Hz), 128.9, 127.6, 118.2 (d, J = 88.0 Hz), 113.1, 66.2, 33.9, 33.5, 32.9, 27.2, 25.6. ^{31}P NMR (162 MHz, $CDCl_3$) δ 20.79. HRMS (ESI), $C_{33}H_{30}ClNO_2PS_2$ calcd for M^+ 602.1139, found 602.1144.

*4.2.11.2. (2-((6-((4-(4-chlorophenyl)thiazol-2-yl)thio)hexyl)oxy)-2-oxoethyl)-triphenylphosphonium bromide (**12b**).* White solid (1.77 g, yield 83 %). ^{1}H NMR (400 MHz, $CDCl_3$) δ 7.74–7.67 (m, 7H), 7.66–7.60 (m, 4H), 7.54–7.48 (m, 6H), 7.31 (s, 1H), 7.16 (d, J = 8.4 Hz, 2H), 5.28 (s, 2H), 3.79 (t, J = 6.4 Hz, 2H), 3.04 (t, J = 7.1 Hz, 2H), 1.55 (p, J = 7.2 Hz, 2H), 1.29–1.16 (m, 4H), 1.05–0.97 (m, 2H). ^{13}C NMR (100 MHz, $CDCl_3$) δ 164.8, 164.0, 153.5, 134.9 (d, J = 2.9 Hz), 133.5 (d, J = 10.7 Hz), 133.3, 132.3, 129.9 (d, J = 13.2 Hz), 128.4, 127.2, 117.5 (d, J = 88.9 Hz), 112.9, 66.3, 34.0, 32.7 (d, J = 56.3 Hz), 28.6, 27.7, 27.6, 24.8. ^{31}P NMR (162 MHz, $CDCl_3$) δ 20.8. HRMS (ESI), $C_{35}H_{34}ClNO_2PS_2$ calcd for M^+ 630.1452, found 630.1457.

*4.2.11.3. (2-((8-((4-(4-chlorophenyl)thiazol-2-yl)thio)octyl)oxy)-2-oxoethyl)triphenyl-phosphonium bromide (**12c**).* White solid (1.77 g, yield 80 %). ^{1}H NMR (400 MHz, $CDCl_3$) δ 7.93–7.84 (m, 6H), 7.78 (dd, J = 18.0, 7.7 Hz, 5H), 7.66 (s, 6H), 7.38–7.32 (m, 3H), 5.56 (d, J = 13.4 Hz, 2H), 3.94 (t, J = 6.7 Hz, 2H), 3.23 (t, J = 7.2 Hz, 2H), 1.76 (d, J = 7.6 Hz, 2H), 1.40 (dd, J = 13.9, 6.7 Hz, 4H), 1.27–1.12 (m, 6H). ^{13}C NMR (100 MHz, $CDCl_3$) δ 165.1, 164.1, 153.6, 135.0, 133.6 (d, J = 10.9 Hz), 133.3, 132.3, 130.0 (d, J = 13.1 Hz), 128.5, 127.3, 117.5 (d, J = 88.9 Hz), 112.8, 66.6, 34.2, 32.8 (d, J = 55.6 Hz), 28.8, 28.5, 28.5, 28.2, 27.7, 25.2. ^{31}P NMR (162 MHz, $CDCl_3$) δ 20.7. HRMS (ESI), $C_{37}H_{38}ClNO_2PS_2$ calcd for M^+ 658.1765, found 658.1770.

4.3. Cell culture

HeLa and HCT-15 cells were cultured in RPMI-1640, PC-3 cells were cultured in F12, MCF-7 cells were cultured in DMEM. The media were supplemented with 10 % fetal bovine serum (FBS) and 1 % penicillin/streptomycin. The cells were incubated at 37 °C with 5 % CO_2.

4.4. In vitro cytotoxic activity (CCK-8 assay)

In vitro cytotoxicity of tested compounds was assessed using the Cell Counting Kit-8 following the manufacturer's protocol. Cancer cells were seeded in 96-well plates at a density of 5000 cells/well for 24 h. Then, the cells were treated with different concentrations of thiazole-TPP conjugates for another 24 h. After the treatment, 10 % CCK-8 solution was added to the 96-well plates and incubated for 3 h. DMSO was used for negative control. The absorbance at 450 nm for CCK-8 assay was measured using a microplate reader (Spectra Max i3x, Molecular Devices). The IC_{50} values were calculated by GraphPad 7.0.

4.5. Colony formation assay

HeLa cells were seeded into a 6-well plate at a density of 100 cells/well. Then, the cells were treated with different concentrations of **12a**. After incubation for 12 days, the cells were fixed with 4 % paraformaldehyde for 30 min and then stained with 0.1 % crystal violet solution for 3 min. The colony numbers were photographed by iBright 1500 imaging system (Thermo Fisher Scientific).

4.6. Measurement of mitochondrial membrane potential

HeLa cells were seeded in a 12-well plate at a density of 1×10^4 cells/well and treated with different concentration of **12a** for 24 h. After the treatment, cells were stained by JC-1 at 37 °C for 20 min following the instructions of manufacturer. Afterwards, the images of samples were captured under fluorescence microscope (Ti2-U, Nikon) and the fluorescence intensity were measured by a Cytation 5 multimode reader (Agilent, BioTek). Degree of mitochondrial depolarization was calculated as red/green fluorescence and normalized to the control group.

4.7. Determination of intracellular reactive oxygen species (ROS)

HeLa cells were seeded in a 6-well plate at a density of 5.0×10^5 cells/well and cultured for 24 h. After the treatment with indicated concentrations of **12a**, A DCFH-DA kit was used for ROS detection according to manufacturer's protocol. The stained cell samples were directly observed fluorescence microscope (Ti2-U, Nikon) at the excitation wavelength of 488 nm and emission wavelength of 525 nm. For flow cytometry evaluation, treated cells were collected and resuspended in DCFH-DA that dissolved in buffer supplied by the kit. The cell samples were eventually analyzed with flow cytometry (FACS Celesta, BD) and data were analyzed with FlowJo 8.0.

4.8. Cell apoptosis analysis

HeLa cells were seeded in 6-well plates at a density of 5.0×10^5 cells/well and cultured for 24 h. Then cells were treated with various concentrations of **12a** for another 24 h. Annexin V-FITC/PI staining was performed in accordance with instructions of manufacturer. Finally, the cells were analyzed by flow cytometry (FACS Celesta, BD) and data were analyzed with FlowJo 8.0.

4.9. Cell cycle assay

HeLa cells were seeded in 6-well plates at a density of 2.0×10^5 cells/well and cultured for 24 h. Then cells were treated with various concentrations of **12a** for another 24 h. PI staining was performed in accordance with instructions of manufacturer. Finally, the cells were analyzed by flow cytometry (NovoCyte, Agilent) and data were analyzed with NoveExpress.

4.10. Mitochondrial bioenergetics assay

The oxygen consumption rate (OCR) and extracellular acidification rate (ECAR) measurements were performed on a Seahorse XFp analyzer. HeLa cells were seeded in 8-well Seahorse XFp microplates at the densities of 4000 cells/well and cultured at room temperature for 1 h for the cells to attach. After incubation overnight, the cells were treated with **12a** (10 μM) for 2 h. OCR was measured using Seahorse XF Mitostress Test Kit (Agilent Technology). When OCR was recorded, oligomycin (ATP synthase inhibitor), FCCP (mitochondrial uncoupler) and the mixture of rotenone (inhibitor of complex I) and antimycin A (inhibitor of complex III) were injected in sequence. ECAR was measured using Seahorse XF Glycolysis Stress Test Kit (Agilent Technology). When ECAR was recorded, glucose, oligomycin and 2-DG were added consecutively.

4.11. Western blot assay

HeLa cells (5.0×10^5 cells/well) were seeded in 6-well plates. After treatment of compound **12a** for 2 h, cells were lysed in the RIPA buffer with protease inhibitor. The protein concentration was determined using the BCA Protein Assay Kit. Total protein (35 μg) were separated by 10 % Bis-Tris gel, transferred to PVDF membranes. And then, the membranes were incubated with different primary antibodies solutions at 4℃ overnight. After being washed with TBST solution, the membranes were incubated with corresponding secondary antibodies. Finally, after incubation with secondary antibody, the protein bands were visualized by a LI-COR Odyssey scanner and analyzed by Image Studio.

4.12. Statistical analysis

Data are presented as mean ± SD (n = 3) and statistically analyzed by GraphPad Prism 7 software. One-way ANOVA was performed for multiple group comparisons.

CRediT authorship contribution statement

Yixin Hu: Data curation, Formal analysis, Investigation, Methodology, Writing – original draft. **Yang Zhang:** Data curation, Formal analysis, Investigation. **Jie Guo:** Data curation, Formal analysis, Investigation. **Shihao Chen:** Data curation, Investigation. **Jie Jin:** Investigation. **Pengyu Li:** Investigation. **Yuchen Pan:** Investigation. **Shuwen Lei:** Investigation. **Jiaqi Li:** Investigation. **Suheng Wu:** Investigation. **Buzhou Bu:** Investigation. **Lei Fu:** Conceptualization, Funding acquisition, Resources, Supervision, Writing – review & editing.

Declaration of competing interest

The authors declare that they have no known competing financial interests or personal relationships that could have appeared to influence the work reported in this paper.

Acknowledgments

This work was supported by the SIP High-Quality Innovation Platform for Chronic Diseases (YZCXPT2022203).

Appendix A. Supplementary data

Supplementary data to this article can be found online at https://doi.org/10.1016/j.bioorg.2024.107588.

References

[1] D. Van, M.M. Sedensky, P.G. Morgan, Cell biology of the mitochondrion, Genetics 207 (2017) 843.
[2] V. Gogvadze, S. Orrenius, B. Zhivotovsky, Mitochondria in cancer cells: what is so special about them? Trends Cell Biol. 18 (2008) 165–173.
[3] I. Martínez-Reyes, N.S. Chandel, Mitochondrial TCA cycle metabolites control physiology and disease, Nat. Commun. 11 (2020) 102.
[4] W. Jie, F. Lin, L.L. Guo, X.J. Xiong, F. Xun, Cardiovascular disease, mitochondria, and traditional chinese medicine, Evid.-Based Complement. Altern. Med. -Ecam 2015 (2015) 143145.
[5] M.T. Lin, M.F. Beal, Mitochondrial dysfunction and oxidative stress in neurodegenerative diseases, Nature 443 (2006) 787–795.
[6] W. Yuanbo, C. Meiqiao, J. Jielong, Mitochondrial dysfunction in neurodegenerative diseases and drug targets via apoptotic signaling, Mitochondrion 49 (2019) 35–45.
[7] B.B. Lowell, G.I. Shulman, Mitochondrial dysfunction and type 2 diabetes, Science 307 (2005) 384–387.
[8] F.G. De Felice, S.T. Ferreira, Inflammation, defective insulin signaling, and mitochondrial dysfunction as common molecular denominators connecting type 2 diabetes to Alzheimer disease, Diabetes 63 (2014) 2262–2272.
[9] L. Guy, F.O. Marcus, S.S. Orian, Emerging roles of β-cell mitochondria in type-2-diabetes, Mol. Aspect. Med. 71 (2020) 100843.
[10] L. Galluzzi, E. Morselli, O. Kepp, I. Vitale, A. Rigoni, E. Vacchelli, M. Michaud, H. Zischka, M. Castedo, G. Kroemer, Mitochondrial gateways to cancer, Mol. Aspect. Med. 31 (2010) 1–20.
[11] D.C. Wallace, Mitochondria and cancer, Nat. Rev. Cancer 12 (2012) 685–698.
[12] R. Gundamaraju, W. Lu, R. Manikam, Revisiting mitochondria scored cancer progression and metastasis, Cancers 13 (2021) 432.
[13] O. Warburg, On the origin of cancer cells, Science 123 (1956) 309–314.
[14] H. Douglas, A.W. Robert, Hallmarks of cancer: The next generation, Cell 144 (2011) 646–674.
[15] S.-M.-N. Josephine, K.S. Keshav, Mitochondrial dysfunction in cancer, Mitochondrion 4 (2004) 755–762.
[16] V. Sejal, Z. Elma, C.H. Marcia, Mitochondria and cancer, Cell 166 (2016) 555–566.

[17] Q.C. Xiao, W. Du, X. Dong, S.B. Du, S.Y. Ong, G.H. Tang, C.Y. Zhang, F. Yang, L. Li, L.Q. Gao, S.Q. Yao, Cell-Penetrating mitochondrion-targeting ligands for the universal delivery of small molecules, proteins and nanomaterials, Chem. Eur. J. 27 (2021) 12207–12214.
[18] J. Zielonka, J. Joseph, A. Sikora, M. Hardy, O. Ouari, J. Vasquez-Vivar, G. Cheng, M. Lopez, B. Kalyanaraman, Mitochondria-targeted triphenylphosphonium-based compounds: Syntheses, mechanisms of action, and therapeutic and diagnostic applications, Chem. Rev. 117 (2017) 10043–10120.
[19] J.S. Modica-Napolitano, J.R. Aprille, Delocalized lipophilic cations selectively target the mitochondria of carcinoma cells, Adv. Drug Deliv. Rev. 49 (2001) 63–70.
[20] M.T. Jeena, S. Kim, S. Jin, J.-H. Ryu, Recent progress in mitochondria-targeted drug and drug-free agents for cancer therapy, Cancers 12 (2020) 4.
[21] C.-J. Zhang, J. Wang, J. Zhang, Y.M. Lee, G. Feng, T.K. Lim, H.-M. Shen, Q. Lin, B. Liu, Mechanism-guided design and synthesis of a mitochondria-targeting artemisinin analogue with enhanced anticancer activity, Angew. Chem. Int. Ed. 55 (2016) 13770–13774.
[22] C.A. Reddy, V. Somepalli, T. Golakoti, A.K. Kanugula, S. Karnewar, K. Rajendiran, N. Vasagiri, S. Prabhakar, P. Kuppusamy, S. Kotamraju, V.K. Kutala, Mitochondrial-targeted curcuminoids: A strategy to enhance bioavailability and anticancer efficacy of curcumin, PLoS One 9 (2014) e89351.
[23] Y. Ye, T. Zhang, H. Yuan, D. Li, H. Lou, P. Fan, Mitochondria-targeted lupane triterpenoid derivatives and their selective apoptosis-inducing anticancer mechanisms, J. Med. Chem. 60 (2017) 6353–6363.
[24] K. Zhang, J. Fu, X. Liu, Y. Guo, M. Han, M. Liu, X. Wang, Mitochondrial-targeted triphenylphosphonium–hydroxycamptothecin conjugate and its nano-formulations for breast cancer therapy: In vitro and in vivo investigation, Pharmaceutics 15 (2023) 388.
[25] M. Millard, J.D. Gallagher, B.Z. Olenyuk, N. Neamati, A selective mitochondrial-targeted chlorambucil with remarkable cytotoxicity in breast and pancreatic cancers, J. Med. Chem. 56 (2013) 9170–9179.
[26] D. Huang, Q. Liu, M. Zhang, Y. Guo, Z. Cui, T. Li, D. Luo, B. Xu, C. Huang, J. Guo, K.Y. Tam, M. Zhang, S.-L. Zhang, Y. He, A Mitochondria-targeted phenylbutyric acid prodrug confers drastically improved anticancer activities, J. Med. Chem. 65 (2022) 9955–9973.
[27] K. Sunwoo, M. Won, K.-P. Ko, M. Choi, J.F. Arambula, S.-G. Chi, J.L. Sessler, P. Verwilst, J.S. Kim, Mitochondrial relocation of a common synthetic antibiotic: A non-genotoxic approach to cancer therapy, Chem 6 (2020) 1408–1419.
[28] D. Xin, L. Shuwen, L. Shuhua, H. Yixin, W. Juntao, Z. Dongdong, L. Dan, J. Faqin, F. Lei, Design, synthesis and biological evaluation of novel thiazole-derivatives as mitochondrial targeting inhibitors of cancer cells, Bioorg. Chem. 114 (2021) 105015.
[29] L. Shuhua, D. Xin, W. Juntao, Y. Chang, H. Yixin, L. Shuwen, Z. Yang, L. Dan, J. Faqin, F. Lei, Biological evaluation of mitochondria targeting small molecules as potent anticancer drugs, Bioorg. Chem. 114 (2021) 105055.
[30] L. Ma, X. Wang, W. Li, T. Li, S. Xiao, J. Lu, J. Xu, Y. Zhao, Rational design, synthesis and biological evaluation of triphenylphosphonium-ginsenoside conjugates as mitochondria-targeting anti-cancer agents, Bioorg Chem. 103 (2020) 104150.
[31] J.H. Francisco, P. Adrián, D. Jelena, P. Milica, M.P. José, L. Óscar, G.-F.-B. José, Straightforward access to novel mitochondriotropics derived from 2-arylethanol as potent and selective antiproliferative agents, Eur. J. Med. Chem. 228 (2022) 113980.
[32] M. Clelia, C. Quentin, T. Thi, N. Delphine, M.-B. Florence, A. Mouad, F. Elias, M. Samir, V.-G. Juliette, Synthesis and antiproliferative activity of 6BrCaQ-TPP conjugates for targeting the mitochondrial heat shock protein TRAP1, Eur. J. Med. Chem. 229 (2022) 114052.
[33] H. Li, A. Lu, Y. Zhang, Y. Peng, G. Song, Synthesis of novel azabicyclo derivatives containing a thiazole moiety and their biological activity against pine-wood nematodes, Phosphorus Sulfur Silicon Relat. Elem. 195 (2020) 371–375.
[34] D. Nolfi-Donegan, A. Braganza, S. Shiva, Mitochondrial electron transport chain: Oxidative phosphorylation, oxidant production, and methods of measurement, Redox Biol. 37 (2020) 101674.
[35] D. Trachootham, J. Alexandre, P. Huang, Targeting cancer cells by ROS-mediated mechanisms: A radical therapeutic approach? Nat. Rev. Drug Discov. 8 (2009) 579–591.
[36] J. Liu, Z. Wang, Increased oxidative stress as a selective anticancer therapy, Oxid. Med. Cell. Longev. 2015 (2015) 294303.
[37] H. Wang, J.A. Joseph, Quantifying cellular oxidative stress by dichlorofluorescein assay using microplate reader, Free Radic. Biol. Med. 27 (1999) 612–616.
[38] J.H. Kim, S. Ofori, S. Parkin, H. Vekaria, P.G. Sullivan, S.G. Awuah, Anticancer gold(iii)-bisphosphine complex alters the mitochondrial electron transport chain to induce in vivo tumor inhibition, Chem. Sci. 12 (2021) 7467–7479.
[39] A.S. Arojojoye, C. Olelewe, S. Gukathasan, J.H. Kim, H. Vekaria, S. Parkin, P. G. Sullivan, S.G. Awuah, Serum-stable gold(III) bisphosphine complex induces mild mitochondrial uncoupling and in vivo antitumor potency in triple negative breast cancer, J. Med. Chem. 66 (2023) 7868–7879.
[40] E.C. Weinbach, J. Garbus, Mechanism of action of reagents that uncouple oxidative phosphorylation, Nature 221 (1969) 1016–1018.
[41] S. Demine, P. Renard, T. Arnould, Mitochondrial uncoupling: A key controller of biological processes in physiology and diseases, Cells 8 (2019) 795.
[42] T. Okamoto, T. Shimada, C. Matsumura, H. Minoshima, T. Ban, M. Itotani, T. Shinohara, S. Fujita, S. Matsuda, S. Sato, N. Kanemoto, New approach to drug discovery of a safe mitochondrial uncoupler: OPC-163493, ACS Omega 6 (2021) 16980–16988.
[43] I.L. Paraiso, L.M. Mattio, A. Alcázar Magaña, J. Choi, L.S. Plagmann, M.A. Redick, C.L. Miranda, C.S. Maier, S. Dallavalle, C. Kioussi, P.R. Blakemore, J.F. Stevens, Xanthohumol pyrazole derivative improves diet-induced obesity and induces energy expenditure in high-fat diet-fed mice, ACS Pharmacol. Transl. Sci. 4 (2021) 1782–1793.
[44] J.H. Murray, A.L. Burgio, M. Beretta, S.R. Hargett, T.E. Harris, E. Olzomer, R. J. Grams, C.J. Garcia, C. Li, J.M. Salamoun, K.L. Hoehn, W.L. Santos, Oxadiazolopyridine derivatives as efficacious mitochondrial uncouplers in the prevention of diet-induced obesity, J. Med. Chem. 66 (2023) 3876–3895.
[45] J.A. Jara, V. Castro-Castillo, J. Saavedra-Olavarría, L. Peredo, M. Pavanni, F. Jaña, M.E. Letelier, E. Parra, M.I. Becker, A. Morello, U. Kemmerling, J.D. Maya, J. Ferreira, Antiproliferative and uncoupling effects of delocalized, lipophilic, cationic gallic acid derivatives on cancer cell lines. Validation in vivo in singenic, J. Med. Chem. 57 (2014) 2440–2454.
[46] L. Yapeng, L. Siyuan, W. Ying, W. Dang, G. Jing, Z. Li, Asiatic acid uncouples respiration in isolated mouse liver mitochondria and induces HepG2 cells death, Eur. J. Pharmacol. 786 (2016) 212–223.
[47] W. Zhang, V.M. Sviripa, L.M. Kril, T. Yu, Y. Xie, W.B. Hubbard, P.G. Sullivan, X. Chen, C.-G. Zhan, Y. Yang-Hartwich, B.M. Evers, B.T. Spear, R. Gedaly, D. S. Watt, C. Liu, An underlying mechanism of dual Wnt inhibition and AMPK activation: Mitochondrial uncouplers masquerading as Wnt inhibitors, J. Med. Chem. 62 (2019) 11348–11358.
[48] E.R.M. Zunica, C.L. Axelrod, E. Cho, G. Spielmann, G. Davuluri, S.J. Alexopoulos, M. Beretta, K.L. Hoehn, W.S. Dantas, K. Stadler, W.T. King, K. Pergola, B.A. Irving, I.M. Langohr, S. Yang, C.L. Hoppel, L.A. Gilmore, J.P. Kirwan, Breast cancer growth and proliferation is suppressed by the mitochondrial targeted furazano[3,4-b]pyrazine BAM15, Cancer Metab. 9 (2021) 36.
[49] R. Shrestha, E. Johnson, F.L. Byrne, Exploring the therapeutic potential of mitochondrial uncouplers in cancer, Mol. Metabol. 51 (2021) 101222.
[50] E.S. Childress, S.J. Alexopoulos, K.L. Hoehn, W.L. Santos, Small molecule mitochondrial uncouplers and their therapeutic potential, J. Med. Chem. 61 (2018) 4641–4655.
[51] M.K. Brandon, L.W. Janelle, B. Amandeep, K.P. Ivan, L.B. Frances, A.M. Beverley, A.C. Joseph, H. Liping, S.D. Ajit, L.T. Jose, O. Kohki, H.L. Ryan, C. Linda, Y. Zhen, J.S. Jeffrey, S.S. Jeffrey, W.H. Jeffrey, R.L. Kevin, S.R. Kodi, U. Seiichi, L. S. Webster, W.R. George, D.O. Mark, A.B. Douglas, L.H. Kyle, Identification of a novel mitochondrial uncoupler that does not depolarize the plasma membrane, Mol. Metabol. 3 (2014) 114–123.
[52] T. Nie, S. Zhao, L. Mao, Y. Yang, W. Sun, X. Lin, S. Liu, K. Li, Y. Sun, P. Li, Z. Zhou, S. Lin, X. Hui, A. Xu, C.W. Ma, Y. Xu, C. Wang, P.R. Dunbar, D. Wu, The natural compound, formononetin, extracted from Astragalus membranaceus increases adipocyte thermogenesis by modulating PPARγ activity, Br. J. Pharmacol. 175 (2018) 1439–1450.
[53] A.M. Bertholet, A.M. Natale, P. Bisignano, J. Suzuki, A. Fedorenko, J. Hamilton, T. Brustovetsky, L. Kazak, R. Garrity, E.T. Chouchani, N. Brustovetsky, M. Grabe, Y. Kirichok, Mitochondrial uncouplers induce proton leak by activating AAC and UCP1, Nature 606 (2022) 180–187.
[54] J. Petr, J. Martin, K.P. Richard, Uncoupling mechanism and redox regulation of mitochondrial uncoupling protein 1 (UCP1), Biochim. Biophys. Acta Bioenerg. 1860 (2019) 259–269.
[55] W. Xiao, Z. Xiong, W. Xiong, C. Yuan, H. Xiao, H. Ruan, Z. Song, C. Wang, L. Bao, Q. Cao, K. Wang, G. Cheng, T. Xu, J. Tong, L. Zhou, W. Hu, Z. Ru, D. Liu, H. Yang, X. Zhang, K. Chen, Melatonin/PGC1A/UCP1 promotes tumor slimming and represses tumor progression by initiating autophagy and lipid browning, J. Pineal Res. 67 (2019) e12607.
[56] J. Xia, C. Chu, W. Li, H. Chen, W. Xie, R. Cheng, K. Hu, X. Li, Mitochondrial protein UCP1 inhibits the malignant behaviors of triple-negative breast cancer through activation of mitophagy and pyroptosis, Int. J. Biol. Sci. 18 (2022) 2949–2961.
[57] F. Zhang, B. Liu, Q. Deng, D. Sheng, J. Xu, X. He, L. Zhang, S. Liu, UCP1 regulates ALDH-positive breast cancer stem cells through releasing the suppression of Snail on FBP1, Cell Biol. Toxicol. 37 (2021) 277–291.
[58] M. Balti, A. Plas, C. Meinguet, M. Haufroid, Q. Thémans, M.L. Efrit, J. Wouters, S. Lanners, Synthesis of 4- and 5-arylthiazolinethiones as inhibitors of indoleamine 2,3-dioxygenase, Bioorg. Med. Chem. Lett. 27 (2017) 3607–3610.